Title: Ammonium regulates the development and architecture of pine roots through hormonal crosstalk and differential expression of transcription factors in the apex

Authors: Francisco Ortigosa[1], César Lobato-Fernández[1], Hitomi Shikano[2], Concepción Ávila[1], Shu Taira[2], Francisco M. Cánovas[1], Rafael A. Cañas[1,3]*.

Affiliation: [1]Grupo de Biología Molecular y Biotecnología de Plantas, Departamento de Biología Molecular y Bioquímica, Universidad de Málaga, Campus Universitario de Teatinos, 29071-Málaga, Spain

[2]Faculty of Food and Agricultural Sciences, Fukushima University, Kanayagawa, Fukushima 960-1296, Japan.

[3]Integrative Molecular Biology Lab, Universidad de Málaga, Campus Universitario de Teatinos, 29071-Málaga, Spain

***Correspondence:** Rafael A. Cañas, Departamento de Biología Molecular y Bioquímica, Facultad de Ciencias, Universidad de Málaga, Campus Universitario de Teatinos s/n, E-29071 Málaga, Spain. e-mail: rcanas@uma.es Phone number: +34-925-131673 Fax number: +34-952-132041.

ORCID: FO (0000-0002-7517-7594); CLF (0000-0001-9576-7236); HS (0000-0001-8973-3355); CA (0000-0001-8817-7529); ST (0000-0002-9243-0395); FMC (0000-0002-4914-2558) and RAC (0000-0001-9727-5585)

SUMMARY

Ammonium is a prominent source of inorganic nitrogen for plant nutrition, but excessive amounts can be toxic for many species. However, most conifers are tolerant to ammonium, a relevant physiological feature of this ancient evolutionary lineage. For a better understanding of the molecular basis of this trait, ammonium-induced changes in the transcriptome of maritime pine (*Pinus pinaster* Ait.) root apex have been determined by laser capture microdissection and RNA sequencing. Ammonium promoted changes in the transcriptional profiles of multiple transcription factors, such as *SHORT-ROOT*, and phytohormone-related transcripts, such as *ACO*, involved in the development of the root meristem. Nano-PALDI-MSI and transcriptomic analyses showed that the distributions of IAA and CKs were altered in the root apex in response to ammonium nutrition. Taken together, the data suggest that this early response is involved in the increased lateral root branching and principal root growth, which characterize the long-term response to ammonium supply in pine. All these results suggest that ammonium induces changes in the root system architecture through the IAA-CK-ET phytohormone crosstalk and transcriptional regulation.

KEYWORDS: Transcriptomics; conifer; *Pinus pinaster*; nitrogen nutrition; laser capture microdissection; root development; phytohormones

INTRODUCTION

Nitrogen (N) is a vitally important nutrient for all living organisms because it is a constituent of essential biomolecules such as nucleic acids, proteins, amino acids, porphyrins and hormones, among others (Miller and Cramer, 2005). This nutrient is indispensable for the proper growth and development of plants, and it can be assimilated from different kinds of sources, including organic (peptides, amino acids, and urea) and inorganic (nitrate and ammonium) forms (Näsholm *et al.,* 1998, Hachiya and Sakakibara, 2017). Together with nitrate (NO_3^-), ammonium (NH_4^+) is one of the main forms of inorganic N available for plants, and the relative proportions of these elements in soil can vary depending on biological and climate conditions (Bijlsma *et al.,* 2000). NH_4^+ at millimolar levels usually causes toxicity in most plants. Among the effects caused by an excessive NH_4^+ include decreased plant growth, leaf chlorosis, decreased root/shoot ratios, decreased root gravitropism and altered the root system architecture (RSA) (Esteban *et al.,* 2016). Regarding the changes in RSA, the inhibition of root elongation and enhancement of lateral root (LR) formation are commonly observed (Y. Liu and von Wirén, 2017).

Root elongation involves three interconnected biological processes intervene: cell division, cell expansion and cell differentiation (Youssef *et al.,* 2018). Auxins (IAAs) play a prominent role in the first two processes (Wang and Ruan, 2013) and can be synthesized in the root meristem and transported toward upstream adjacent regions through specific transporters, such as AUXIN RESPONSE 1 (AUX1) and PINFORMED 1-7 (PIN1-7) (Grunewald and Friml, 2010). IAAs induce the expression of PLETHORA 1-4 (PLT1-4) transcription factors (TFs) in the root meristem, which are responsible for cell proliferation maintenance (Galinha *et al.,* 2007). Other TFs have been described to play key roles in the stem cell niche and the quiescent center (QC) maintenance to produce all tissues required to form a mature root, including the TFs SHORT-ROOT (SHR) and SCARECROW (SCR) (Sablowski, 2011). SHR expression is localized in a zone of the stele that constitutes the central part of the root and stem (Miyashima *et al.,* 2011; Kim *et al.,* 2020). When *SHR* transcripts are translated, SHR proteins move into adjacent cells (pericycle cells, endodermis, QC and phloem pole) to activate the expression of SCR (Helariutta *et al.,* 2000; Nakajima *et al.,* 2000; Sena *et al.,* 2004; Cui *et al.,* 2007). SHR also plays key roles in phloem development, controlling the asymmetric cell division process for sieve element development by the regulation of NARS1 and SND2 NAC-type TFs (Kim *et al.,* 2020).

This fact is relevant because these cell types constitute the phloem (Greb, 2020), which is the main means of IAA transport (Chapman and Estelle, 2009). Under the presence of NH_4^+, IAAs can influence root growth inhibition, root agravitropic response and LR branching (Cao *et al.,* 1993; Y. Liu *et al.,* 2013; Araya *et al.,* 2016). However, Y. Liu *et al.* (2013) showed that NH_4^+ does not affect the IAA content at QC, where the maximum level of this phytohormone in roots is localized (Zhou *et al.,* 2010). In *Arabidopsis,* root growth inhibition in response to NH_4^+ represses root cell production by decreasing the meristem size and the number of dividing cells without altering the cell division rate. Furthermore, NH_4^+ also decreases the number of root cap cells (Y. Liu *et al.,* 2013). In this sense, several TFs have been described to play key roles in root cap development, such as BEARSKIN (BRN) and SOMBRERO (SMB) (Bennett *et al.,* 2010, 2014; Kamiya *et al.,* 2016). However, the transcriptional pathway regulating NH_4^+ root cap development has not yet been deciphered.

On the other hand, NH_4^+ inhibits the gravitropic response by downregulating the expression of AUX1 and PIN2, which are two pivotal IAA transporters (Y. Liu *et al.,* 2013). LR branching is enhanced by under a supply of NH_4^+ (Araya *et al.,* 2016). When the quadruple ammonium transporter (AMT) knockout lines were complemented with *AtAMT1.1* or *AtAMT1.3*, only *AtAMT1.3*-complemented plants were able to restore the LR branching phenotype induced by NH_4^+ (Lima *et al.,* 2010), suggesting that the NH_4^+-induced LR branching signaling events are dependent on AtAMT1.3 (Lima *et al.,* 2010). In addition, IAAs have been suggested to be involved in this signaling event due to the repression of PIN2 under a supply of NH_4^+ (Y. Liu *et al.,* 2013; Zou *et al.,* 2013). This evidence describes the importance of IAA in orchestrating the root system configuration in response to this nutritional stimulus. However, the transcriptional regulatory mechanisms that control this response remain unclear.

Together with IAAs, cytokinins (CKs) have been previously established to be important in root plant growth and vascular development (Kamada-Nobusada *et al.,* 2013; Miyashima *et al.,* 2019; Mao *et al.,* 2020). CK biosynthesis and activity in plants are closely related to N availability (Takei *et al.,* 2004; Kamada-Nobusada *et al.,* 2013). In the roots of rice, NH_4^+ nutrition leads to the accumulation of different CKs and CK-derived compounds (Kamada-Nobusada *et al.,* 2013). During active growth of *Arabidopsis*, the content of CKs first increased in the vascular system, thus reflecting CKs transport from roots to shoots

(Shtratnikova *et al.,* 2015). Recently, it has been reported that CK signaling in the early protophloem-sieve-element cell files of *Arabidopsis* root procambial tissue promotes the expression of several DOF TFs (Miyashima *et al.,* 2019). Together with the IAA-responsive dependent HD-ZIP III proteins, these TFs compose a transcriptional network that integrates spatial information of the hormonal domains and miRNA gradients, which are essential for root vascular development (Miyashima *et al.,* 2019).

Conifers are an ancient group of gymnosperms that cover vast regions in the Northern Hemisphere, and they have exceptional ecologic and socioeconomic importance (Farjon *et al.,* 2018). Since conifers represent a differentiated evolutionary lineage of plants, they exhibit substantial differences in N metabolism with respect to angiosperms such as *Arabidopsis*. For instance, conifers lack glutamine biosynthesis in the plastid of photosynthetic cells (Cánovas *et al.,* 2007), and most species prefer NH_4^+ over NO_3^- as the main source of inorganic N (Kronzucker *et al.,* 1997; Hawkins and Robbins, 2010). This is the case for maritime pine (*Pinus pinaster* Aiton) (Warren and Adams, 2002; Ortigosa *et al.,* 2020), a southwestern Mediterranean conifer employed as a model in studies of N nutrition and metabolism and for which a large body of genomics resources are available (Cañas *et al.,* 2017; Ortigosa *et al.,* 2020, 2021). In maritime pine roots, a supply of NH_4^+ induced the expression of transcripts related to defense, such as *antimicrobial peptide 1* (*PpAMP1*) (Canales *et al.,* 2010), which is not found in dicots and can regulate the NH_4^+ uptake (Canales *et al.,* 2011). Additionally, NH_4^+ promotes changes in the epitranscriptome that mainly regulate the translational response and growth, including the repression of 1-aminocyclopropane-1-carboxylic acid (ACC) oxidase (ACO), the last enzyme in the ethylene (ET) biosynthesis pathway (Ortigosa *et al.,* 2021). Considering this background, the main goal of the present work was to decipher the molecular mechanisms underlying the early response to NH_4^+ in the root apex and its relationship with root development in maritime pine.

MATERIALS AND METHODS

Plant material

Maritime pine seeds (*P. pinaster* Aiton) from "Sierra Segura y Alcaraz" (Albacete, Spain) were provided by the *Área de Recursos Genéticos Forestales* of the Spanish *Ministerio de Agricultura, Pesca y Alimentación*. Seed germination was carried out following the protocol described elsewhere (Cañas *et al.*, 2006). Seedlings were grown in vermiculite in plant growth chambers (Aralab Fitoclima 1200, Rio de Mouro, Portugal) under 16 h light photoperiod, a luminal intensity of 125 $\mu mol\ m^{-2}\ s^{-1}$, a constant temperature of 23 °C and watered twice a week with distilled water. One-month-old maritime pine seedlings were used for the experiments. Pine seedlings were randomly subdivided into three different groups, relocated into forestall seedbeds and irrigated with 80 mL of a solution that contains macro- and micronutrients without any N source (1.16 mM KCl; 0.63 mM KH_2PO_4; 0.35 mM $MgSO_4 \cdot 7H_2O$; 0.17 mM $CaCl_2 \cdot H_2O$; 80 μM EDTA-$FeSO_4$; 25.9 μM H_3BO_3; 10.2 μM $MnCl_2 \cdot 4H_2O$; 1.3 μM $ZnSO_4 \cdot 7H_2O$; 0.7 μM $CuSO_4 \cdot 5H_2O$; 0.1 μM $Na_2MoO_4 \cdot 2H_2O$). After three days of acclimation, the control group was irrigated with 80 mL of water and the experimental group was supplied with 80 mL of 3 mM NH_4Cl. Root samples were collected 24 h after the treatment and immediately frozen in liquid N (Fig. 1). Ten seedlings were collected and pooled per each sample. The same experiment was carried out three independent times. The screening condition and adequate development of each experiment was verified through the gene expression analysis by RT-qPCR of control genes following previous results (Ortigosa *et al.*, 2021) (Fig. 1). To perform laser capture microdissection (LCM), seedling's root apex were cut, and tissues (5-6 mm) were imbibed in a specimen holder with Tissue-Tek optimal cutting temperature embedding medium (Sakura Finetek, Alphen aan den Rijn, The Netherlands) and immediately frozen in liquid N for cryostat sectioning. Frozen samples were stored at -80°C until use.

For the root phenotypes under different nitrogen sources (NH_4^+ and NO_3^-), the pine seedlings were cultivated in a growth chamber with a 16/8 h light/dark photoperiod, light intensity of 125 $\mu mol\ m^{-2}\ s^{-1}$, constant temperature of 23°C, and 50% relative humidity (Aralab Fitoclima 1200, Rio de Mouro, Portugal). One-month-old seedlings (n = 30) were randomly transplanted into seedbeds for each experimental condition: distilled water, 3 mM KNO_3 and 3 mM NH_4Cl. Each experimental condition group was irrigated twice per week with 50 mL of the corresponding N solution or 50 mL of distilled water for 74 days. After

treatment, seedling roots were dissected and whole roots, primary root (PR) and LRs were weighted. The PR length and number of LRs was manually assessed (Fig. S1).

Whole root RNA isolation

Total RNA from roots of maritime pine seedlings was isolated following the protocol described by Liao *et al.* (2004) and modified by Canales *et al.* (2012). RNA concentration and purity were determined spectrophotometrically using a Nanodrop ND-1000 (Thermo Scientific, Waltham, MA, USA). Purity of the preparation was assessed by determining the 260/280 and 260/230 ratios. The integrity was assessed by electrophoresis.

Laser capture microdissection, RNA isolation and low-input RNA-seq

LCM procedure was carried through as previously described (Cañas et al., 2014). Full step protocol is described in Methods S1. Four different tissue areas were isolated by microdissection corresponding to the root cap (RC), meristem (RM), developing cortex (RDC) and developing vessels (RDV) areas (Video S1).

All RNA extractions from the microdissection procedure were carried out using manufacturer's instruction protocol (non-LCM) for the RNAqueous-Micro RNA Isolation Kit (Ambion, Austin, TX, USA). RNA quality, DNA contamination and first quantification were performed via RNA Pico Assay for the 2100 Bioanalyzer (Agilent, Santa Clara, CA, USA). Quantification was verified via a Qubit RNA BR (Broad-Range) Assay Kit (Invitrogen, Paisley, UK). RNA samples with RNA integrity number (RIN) higher than 7 were used for subsequent RNA sequencing, mRNA amplification and cDNA synthesis 1 ng of RNA for each sample.

The low input RNA-seq was carried out by Novogen (Hong Kong). The cDNA synthesis and amplification, and the library preparation was made with the SMART-Seq™ v4 Ultra™ Low Input RNA Kit for Sequencing (Takara, Mountain View, CA, USA) following the manufacturer's instructions. RNA sequencing was made in a NovaSeq 6000 sequencer according to the manufacturer's instructions for paired-end reads (Illumina, San Diego, CA, USA). The 24 samples were sequenced producing paired-end reads of 150 bp length. The sequencing output is shown in the Table S1.

The raw reads were trimmed (quality and contamination) using SeqTrimBB software (https://github.com/rafnunser/seqtrimbb). Only the pairs in which both reads passed the

quality test were further analyzed (Q>20). Trimmed reads are shown in the Table S1. These reads were assembled using Trinity 2.11 (Haas *et al.*, 2013). Contigs lower than 400 pb were eliminated, for the rest of contigs the redundancy was reduced using CD-HIT-EST software (Fu *et al.*, 2012). This transcriptome shotgun assembly project has been deposited at DDBJ/EMBL/GenBank under the accession GJFX00000000. The version described in this paper is the first version, GJFX01000000. The final transcriptome was used as the reference for the read mapping that was performed with BWA using the MEM option (Li and Durbin, 2009). The read count was obtained with the phyton script *sam2counts* (https://github.com/vsbuffalo/sam2counts). Differentially expressed (DE) transcripts were identified using the edgeR package for R, the transcripts were normalized by cpm and filtered; 2 cpm in at least 2 samples (Robinson *et al.*, 2010). Each sample was from a single seedling in a different experimental replicate. The samples were basically grouped by tissue and nutritional condition (Fig. S2), thus only the transcripts with FDR < 0.05 and the three experimental replicates with the same expression sense than the final logFC (positive or negative) were considered as differentially expressed (DE). These RNA-Seq data have been deposited in the NCBI's Gene Expression Omnibus (Edgar *et al.*, 2002) and are accessible through GEO Series with the accession number GSE175587 (https://www.ncbi.nlm.nih.gov/geo/query/acc.cgi?acc= GSE175587).

Total RNA (1 ng) was retrotranscribed and amplified to verify the expression analyses for several DE genes by RT-qPCR. The cDNA synthesis and amplification protocol was carried out using the Conifer RNA Amplification (CRA+) protocol previously described by Cañas *et al.* (2014). Full step protocol is described in Methods S1. The amplification process was monitored using the ERCC RNA Spike-in kit (Thermo Scientific, Waltham, MA, USA) according to manufacturer's instructions. The primers used for cDNA synthesis and amplification are listed in the Table S2.

Functional annotation and enrichment analyses

The assembled transcriptome was functionally annotated with BLAST2GO (Götz *et al.*, 2008) using DIAMOND software with *blastx* option (Buchfink *et al.*, 2015) against the NCBI's plants-*nr* database (NCBI Resource Coordinators, 2016). Blast results were considered valid with e-value < 1.0E-6. Singular enrichment analysis (SEA) of the GO terms was made in the AGRIGO v2.0 web tool under standard parameters using as GO

term reference the whole assembled transcriptome annotation (Tian *et al*., 2017). Representative enriched GO was determined using REVIGO with 0.5 as dispensability cutoff value (Supek *et al*., 2011).

RT-qPCR

The cDNA synthesis was performed using 1 µg of total RNA and iScript™ cDNA Synthesis Kit (Bio-Rad, Hercules, CA, USA) following manufacturer's instructions. The qPCR primers were designed following the MIQE guidelines (Bustin *et al*., 2009). The primers are listed in the Table S2. qPCRs were carried out using 10 ng of cDNA and 0.4 mM of primers and 2X SsoFast^{TM} EvaGreen® Supermix (Bio-Rad, Hercules, CA, USA) in a total volume of 10 µL. Relative quantification of gene expression was performed using thermocycler CFX 384™ Real-Time System, Bio-Rad, Hercules, CA, USA). The qPCR program was as follows: 3 min at 95 °C (1 cycle), 1 s at 95 °C and 5 s at 60 °C (50 cycles) and a melting curve from 60 to 95 °C, to generate the dissociation curve to confirm the specific amplification of each individual reaction. The analyses were carried out as described by Cañas *et al*. (2014) using the MAK3 model in the R package *qpcR* (Ritz & Spiess, 2008). Normalization for gene expression of experimental design viability was performed using geometric mean of two reference genes, a *Saposin-like aspartyl protease* (pp_199988) and *Myosin heavy chain-related* (pp_58489) that were previously tested for maritime pine (Granados *et al.*, 2016). Normalization for gene expression of LCM isolated tissues was performed using as reference gene a *SKP1/ASK1 family protein* (pp_18128) that was previously tested for maritime pine LCM samples (Granados *et al.*, 2016). For the RT-qPCR analysis, three technical replicates of each sample and three biological replicates were made.

Imaging of phytohormones in roots sections

The main phytohormones were localized in root apex cuts using nano-particle assisted laser desorption/ionization mass spectrometry imaging (Nano-PALDI-MSI). The elongation zones, which corresponded to the region from 2.5 - 5 mm of the root apex, were embedded in super cryoembedding medium (SCEM, Leica Biosystems, Wetzlar, Germany) and frozen in liquid nitrogen. The specimen block was cut into 10 µm sections using a cryostat (NX-70, Thermo Scientific, Waltham, MA, USA) set at -23°C in the chamber and at -25°C on

the object holder. The sections were gently mounted on slides coated with indium tin oxide (ITO) (Bruker Daltonik GmbH, Billerica, MA, USA). Optical images of the sections were obtained by a virtual slide scanner (Nanozmmer-SQ, Hamamatsu Photonics, Shizuoka, Japan) before analysis by Nano-PALDI-MSI.

For Nano-PALDI-MSI, iron oxide-based nanoparticles (Fe-NPs) were prepared by stirring aqueous solutions of $FeCl_2 \cdot 4H_2O$ (5 mL, 100 mM; FUJIFILM Wako Pure Chemical), and 3-aminopropyltriethoxysilane (5 mL; γ-APTES; Shin-Etsu Chemical, Tokyo, Japan) at room temperature for 1 h. The resulting precipitate was washed several times with ultrapure water, resuspended in methanol (Moritake *et al.*, 2007).

One milligram of Fe-NPs was resuspended in 1 mL methanol and sprayed on pine root tissue sections on ITO-coated glass slides with an airbrush (nozzle caliber, 0.2 mm). To obtain images, each data point on the section were irradiated with 200 laser shots in the positive ion detection mode of the mass spectrometer. Only signals between 80 and 800 *m/z* were analyzed to detect the corelated IAA (*m/z* 176.3), cytokinin (*m/z* 221.3), ACC (*m/z* 102.8), salicylic acid (*m/z* 139.4), JA (*m/z* 211.0) and ABA (*m/z* 265.0) as protonated ions, respectively. For each section, approximately 101,800 data points were obtained, 5 μm apart. The MS image was reconstructed from the obtained MS spectra with a mass bin width of m/z ± 0.1 from the exact mass using flexImaging 4.0 (Bruker Daltonik GmbH). The accurate mass of the ions was used for image generation, and mass accuracy and root-mean- square error (RMSE) were automatically calculated by the imaging software to avoid false-positive signals (Shiono and Taira, 2020). Comparisons of MS images were derived from the relative intensity for each signal normalized by the highest intensity spot on the slide.

Phylogenetic analyses

Evolutionary analyses were performed in MEGA7 (Kumar *et al.*, 2016). The protein sequence alignment was made with Muscle (Edgar, 2004). The evolutionary history was inferred using the Neighbor-Joining method (Saitou and Nei, 1987). The bootstrap consensus tree inferred from 1000 replicates is taken to represent the evolutionary history of the taxa analyzed (Felsenstein, 1985).

RESULTS

Tissue-specific transcriptomic response to NH_4^+ supply

In this study, tissue-specific transcriptome changes triggered by NH_4^+ nutrition were analyzed in the maritime pine root apex by a combination of laser capture microdissection and high-throughput RNA sequencing. As described in the Materials and methods section, root apexes from seedlings that were irrigated with 3 mM NH_4^+ and harvested at 24 h were used for the isolation of four different tissues by LCM, namely, RC, RM, RDC and RDV (Video S1). The differential expression results are shown in Dataset S1. A total of 295 DE transcripts were identified in the low-input RNA-seq analysis (Fig. 2a,b), of which 182 DE transcripts were downregulated (Fig. 2a) and 113 were upregulated (Fig. 2b). Among the isolated tissues, RDC showed the highest number of DE transcripts (107 upregulated and 70 downregulated) while RDV had the lowest response (12 upregulated transcripts). Interestingly, only 2 genes were upregulated in all root tissues, namely, two splicing isoforms from a common gene with unknown function.

The analysis of the DE transcripts revealed 8 expression patterns (Fig. 2c). Among the groups with the most significant differences, the cluster 2 had transcripts repressed in RC by NH_4^+, and it contained several TFs, such as *PpSHR*, *PpDOF11* and *PpGATA20-like*, and transcripts related to phytohormones, such as *PpVAN3/FKD2*(Fig. 2c) (Dataset S2). In cluster 3, transcripts related to root development, such as *PpBAM1*, and phytohormones such as *flavanone 3-dioxygenase*, were found to be repressed by NH_4^+ in RC and RDC (Fig. 2c; Dataset S2). In RDC and RM, NH_4^+ induced the transcripts framed into cluster 4, which are mainly related to defense, such as chitinases of class I and IV (Fig. 2c; Dataset S2).

To validate our transcriptomic analysis, the expression value of several DE transcripts was corroborated by RT-qPCR (Fig. 2d; Dataset S1). The downregulation of *PpSHR* (pp_346622) and *PpNPF3.1* (pp_58258) in RC; *PpDOF12* (pp_85381) and *PpACO* (pp_202153) in RM; and *PpBLISTER-like* (pp_170664) in RDC was confirmed. The upregulation of transcripts coding a *cycloeucalenol cycloisomerase* (*PpCPI1*; pp_189071) in RC and *PpAMP1* (pp_580007) in RDC was also corroborated.

Functional enrichment analysis

The functional study of DE transcripts, including the SEA results, is summarized in Fig. 3. In the most responsive tissues (RC, RM and RDC), NH_4^+ induced a general alteration in the amounts of transcripts coding TFs involved in development (most of them downregulated) and transcripts related to different phytohormones (Fig. 3a-c). In the less responsive tissue (RDV) but also in RM and RDC, NH_4^+ promoted the accumulation of defense-related transcripts (Fig. 3b-d). In the SEA results, no significant GO terms were found for DE transcripts upregulated in RC and RDV and downregulated in RM and RDV. The complete results of the SEA analyses are shown in Dataset S3. The most complex SEA results were for transcripts downregulated in RC and upregulated in RDC. The downregulated transcripts in RC were significantly enriched in GO terms in the biological process (BP) category, such as "biological regulation" (GO:0065007), "gene expression" (GO:0010467), "response to hormone" (GO:0009725), "regulation of hormone levels" (GO:0010817) and "regulation of transcription, DNA-templated" (GO:0006355) (Fig. 3e). The terms enriched in the molecular function (MF) category included "transcription factor activity" (GO:0003700), "protein binding" and "DNA binding" (GO:0005515 and GO:0003677) (Fig. 3f). In the BP category for the downregulated transcripts in RDC only the "cytoskeleton organization" term (GO:0007010) was significantly enriched; however, for the upregulated transcripts in this tissue, numerous enriched functions were significant, such as those involved in defense responses such as "induction of programmed cell death" (GO:0012502), "cell killing" (GO:0001906), "defense response" (GO:0006952) and "cell wall macromolecule catabolic process" (GO:0016998) and "amino sugar catabolic process" (GO:0046348) (Fig. 3e). Regarding the MF category for the upregulated transcripts in RDC, there were significant GO terms related to the response to biotic stress, such as "chitinase activity" (GO:0004568), "chitin binding" (GO:0008061), "mannose binding" (GO:0005537) and "hydrolase activity, acting on glycosyl bonds" (GO:0016798) (Fig. 3f). Interestingly, the SEA results of the upregulated transcripts in RM were similar but limited for defense responses, which was also found for the upregulated transcripts in RDC (Fig. 3e,f). Finally, the only enriched GO terms for the cellular component category were "extracellular region" (GO:0005576) and "extracellular space" (GO:0005615) for the transcripts upregulated in RDC tissue (Dataset S3).

Transcription factors affected by NH_4^+ in the apex of maritime pine roots

The DE transcripts were individually analyzed looking to identify different kinds of regulators, such as TFs and transcripts involved in the phytohormone response. From a total of 295 DE transcripts, 31 TFs were identified (Table 1, Dataset S1). All 10 FTs identified in RC were repressed in the presence of NH_4^+. However, in RM and RDC, 6 and 4 TF transcripts were downregulated while 5 and 6 TF transcripts were upregulated, respectively. Interestingly, a high abundance of TFs related to root growth and development was observed (Table 1), such as the strong downregulation of *PpSHR* in RC, *INCURVATA-like* and homeobox-leucine zipper protein *HAT-like* both in RM and involved in meristem developmental regulation, and the TF identified as *zinc finger C2H2 SHOOT GRAVITROPISM* in RC related to the gravitropism response. *PpSHR* was the most highly repressed TF (-11 logFC). Furthermore, the induction of two transcriptional repressors of different plant developmental processes was observed, with *PpNAC31* identified as an *SMB-like* NAC TF in RM and an *OFP17*-like repressor in RDC. In addition, novel TFs in maritime pine were identified. Two of them belong to the DOF-family and were named as *PpDOF11* and *PpDOF12*, and they were both downregulated in RC and RM, respectively. Phylogenetic analysis of these two new DOF-type TFs revealed that *PpDOF11* is grouped with *AtDOF1.4* (AT1G28310) and *OsDOF7.2* (LOC_Os07g32510) into subfamily E and that *PpDOF12* is grouped with members of subfamily A of *P. pinaster*: *PpDOF4*, *PpDOF7*, *PpDOF8* and *PpDOF10* (Fig. S3, Table S3). Additionally, a member of the NAC family (*PpNAC38)* that was upregulated in RM tissue was identified. This TF has homology to *BRN1* (AT1G33280) (e-value: 7e-96) and *BRN2* (AT4G10350) (e-value: 3e-97) of *Arabidopsis thaliana* and is framed within the NAC subfamily C (Fig. S4, Table S4).

Phytohormone-related genes

Twenty-six DE transcripts related to phytohormone pathways were identified (Table 1), of which 19 were upregulated and 7 were downregulated (Dataset S1). Most of these DE transcripts were related to IAA (Table 1). Some interesting examples are the downregulation of transcripts encoding proteins required for PIN transporters localization, such as VAN3/FKD2 Auxin canalis/PH2 (pp_60103) in RC and the upregulation of a *PpCPI1* (pp_189071) in RC, which is related to PIN transporters endocytosis. In addition, in RDC, the repression of transcripts coding for the IAA receptor TIR1/AFB (pp_238715)

and for a sulfotransferase (pp_208269) with a high similarity degree to SULT202B1 (AT3G45070) (e-value: 5e-72) was observed.

CK-related genes were the second most represented phytohormone-related transcripts, and strong repression of CK riboside 5'-monophosphate phosphoribohydrolase (pp_222714) (-6.9 logFC), a CK-activating enzyme, was observed in RC. However, upregulation of a transcript coding for a CK dehydrogenase (pp_215376), a CK-inactivating enzyme, was also observed in RDC. The repression of transcripts related to brassinosteroids and ethylene (ET) biosynthesis, e.g., cytochrome P450 90B1 (pp_247190) in RDC and *PpACO* (pp_202153) in RM was also observed. In addition, transcripts related to the gibberelin (GA) response and abscisic acid (ABA) biosynthesis were upregulated, such as a GASA gibberellin-regulated cysteine-rich protein (pp_111379) in RDC and two ABA2 coding transcripts that might be involved in ABA biosynthesis (pp_198945, and pp_209084) in RM and RDC.

Phytohormone detection in maritime pine root apex

To corroborate whether NH_4^+ nutrition altered the spatial allocation of several phytohormones as the transcriptomic data suggest, the distribution of multiple phytohormones was determined by Nano-PALDI-MSI in the apex of maritime pine roots (Shiono and Taira, 2020). In comparison to control seedlings, changes in the patterns of IAAs, CK (tZ, *trans*-Zeatin), ACC, ABA, salicylic acid (SA) and jasmonic acid (JA) were observed in the presence of NH_4^+ (Fig. 4 and Fig. S5). In the control plants, an IAA gradient was observed, the maximum level was detected in the most distal area of the principal root apex (Fig. 4a); however, in the NH_4^+-treated roots, the IAA maximum was detected in a more distant zone from the root tip (Fig. 4a). CK (tZ) showed a wide distribution in the roots of control plants (Fig. 4b). In the NH_4^+-treated seedlings, CK was distributed in the outer tissues of the root mainly below the root tip (Fig. 4b). Regarding ET, its precursor ACC was found in a very restricted area of the root tip in control and NH_4^+-treated plants, showing lower detection when plants were supplied with NH_4^+ (Fig. 4c). ABA was detected mainly in the RDC tissue in both control and treated seedlings, and it was higher under NH_4^+ supply and distributed below the root apex (Fig. 4d). SA and JA phytohormone distributions were also affected by the presence of NH_4^+ (Fig. S5a,b). SA was located at the end of the root tip, while JA was also detected in the elongation zone in

control plants. When the seedlings were supplied with NH_4^+, SA showed a vaguer spatial distribution with respect to the observed distribution in the control plants (Fig. S5a) while JA tended to slightly increase in the outermost parts of the root apex ends and disappeared from the elongation zone (Fig. S5b).

Maritime pine root phenotype

Maritime pine root morphological studies showed no differences between treatments regarding whole root biomass accumulation (Fig. 5a). When the weight of the principal roots (PRs) was measured, NH_4^+-fed seedlings exhibited a significant reduction in PR weight compared to water- and NO_3^--treated plants (Fig, 5b) and a statistically higher root length when pine seedlings were supplied with either inorganic nitrogen form (Fig. 5c). Moreover, NH_4^+ promoted an increase in LR number and weight compared to the water and NO_3^- treatments (Fig. 5d,e), although no statistically significant differences were observed regarding LR density (LRD) between treatments (Fig. 5f).

DISCUSSION

Despite the obvious environmental and economic importance of conifers, little is known about their response to diverse nutrients at the molecular and developmental levels. Since they represent an ancient lineage of gymnosperms, conifers are of particular interest from an evolutionary perspective because they have common but also differential responses with angiosperm models. The aim of the present work was to explore the early response of maritime pine to NH_4^+ nutrition in the different tissues of the root apex. For this purpose, tissue isolation was performed by LCM and combined with low-input RNA-seq to determine the local transcriptomic response in the growth area of the root. This strategy avoids the dilution effect of transcripts with low and very localized expression, revealing new genes not previously annotated (Cañas *et al.*, 2017), such as *PpDof11-12* and *PpNAC38*. The response to NH_4^+ in RDC involved the expression of defense-related genes as previously described in maritime pine and other model plants (Fig. 3c,e,f) (Canales *et al.*, 2010; Patterson *et al.*, 2010; Ravazzolo *et al.*, 2020; Ortigosa *et al.*, 2021). Obviously, this response might be linked to the peripheral localization of RDC in the roots since the defense proteins encoded by the expressed transcripts develop their functions in the extracellular media (Dataset S3). Some examples are the upregulation of different *ginkbilobin-like/embryo abundant protein* transcripts (e.g. pp_252647) and the *PpAMP1* (pp58007), which are consistent with results previously reported in maritime pine roots (Canales *et al.*, 2010; Ortigosa *et al.*, 2021).

In angiosperm model plants, NH_4^+ alters RSA by inhibiting root elongation, stimulating LR branching and affecting root hair development (Y. Liu & von Wirén, 2017). RSA principally targets root system processes, such as root elongation, root gravitropism and LR branching, appearing to occur in the root tip (Li *et al.*, 2014). Based on the presented transcriptomic analyses, early root exposure to NH_4^+ caused a wide impact on the expression of TFs related to root growth and development in pine (Fig. 2, Table 1). Thus, NH_4^+ caused a strong repression of *PpSHR* (pp_246622) in RC tissue, a GRAS-type TF involved in the regulation and coordination of root development, including phloem differentiation (Kim *et al.*, 2020). Interestingly, in RDC tissue, it was observed that *PpBAM-like* (pp_19744) transcripts were also severely affected by NH_4^+ (Dataset S1), which is consistent with previous cell-specific transcriptomic profiles observed in *Arabidopsis* (Brady *et al.*, 2007). BAM1/2 kinase receptors are required for SHR-dependent

formative divisions in roots and for the proper CYCD6;1 expression, which is required to promote division in cortex endodermal initial daughter cells (Crook *et al.,* 2020).

Additionally, a progressive reduction in the abundance of IAA efflux carriers (PINs) in *Arabidopsis shr* mutants has been described (Lucas *et al.,* 2011), and NH_4^+ negatively affects the expression of PIN2 and AUX1 coding transcripts (Y. Liu *et al.,* 2013). The expression of genes coding for PIN transporters was not affected in pine roots. However, it was observed that the expression of coding transcripts for proteins involved in IAA transporter localization and components of the IAA signaling pathway were affected by NH_4^+. This is the case for *PpCPI1* (pp_189071), which is upregulated in RC and required for PIN2 endocytosis (Men *et al.,* 2008), and the strong repression of *VAN3/PH2/FKD2* (pp_60103) in RC and RM tissues (Table 2), which is crucial in *Arabidopsis* for the vascular leaf pattern formation by the proper PIN transporter localization (Hou *et al.,* 2010). These results suggest that NH_4^+ triggers an alteration in polar auxin transport (PAT) involving a highly coordinated transcriptomic response between tissues of the pine root. The Nano-PALDI-MSI data confirmed that under a supply of NH_4^+, PAT was impaired, thus promoting a putative local increase in IAA presumably in RC and/or RM tissues where cambial development takes place based on IAA-related transcripts and TF expression (Fig. 4a, Fig. 6). These results differ from those previously described in *Arabidopsis* where the presence of NH_4^+ does not seem to affect the distribution of IAAs in the root tip (Y. Liu *et al.,* 2013). This finding could be related to root vascular development and root cell differentiation since adjustments to IAA flux are involved in root cambium development (Marhava *et al.,* 2018), and SCR, a partner of SHR, is involved in the expression and polar localization of PINs (Xu *et al.,* 2006).

Following this line of argument, it is interesting to mention that four maritime pine DOFs were significantly downregulated: *PpDOF11* (pp_58878) and *PpDOF12* (pp_85381) in RC and RM tissues respectively, and *PpDOF1* (pp_233816) and *PpDOF2* (pp_119525) in RDC (Fig. 2), which were preferentially expressed in tissues close to vascular vessels (Fig. S6-S9). Therefore, it is tempting to suggest that these DOFs may be involved in the development of root vessels, as described for PHLOEM EARLY DOF (PEAR) proteins, which are regulated by CK levels (Miyashima *et al.,* 2019). Interestingly, the CK distribution under NH_4^+ supply (Fig. 4b) correlates with the repression of *CK riboside 5'-monophosphate phosphoribohydrolase* (pp_222714), which is a CK activator, in RC

(Kuroha *et al.*, 2009) and the upregulation of a *CK dehydrogenase* (pp_215376), which is involved in CK degradation (Werner *et al.*, 2003), in RDC (Fig. 3a,c). All these results suggest that NH_4^+ could promote an alteration of CK spatial distribution in maritime pine roots, which could be the reason for the wide repression of DOF TFs in RC and RM tissues and its possible role as regulators of cambium development (Fig. 6). Phytohormone imaging showed that CK and IAA were distributed in different zones under a supply of NH_4^+ (Fig. 4a,b), which was possibly due to the opposite roles of these phytohormones in the root meristem since CK negatively regulates QC specification and functions by modulating the IAA response (Zhang *et al.*, 2013).

Additionally, homeobox-leucine zipper (HD-Zip) and NAC-domain TFs are described to take part during development processes (Ochando *et al.*, 2006; Bennett *et al.*, 2010). In *Arabidopsis*, several HATs play important roles in development including the regulation of meristem and procambial maintenance and/or formation (Prigge *et al.*, 2005; Roodbarkelari and Groot, 2017). Accordingly, two HD-Zip coding transcripts identified as *HAT-like* (pp_141831) and *INCURVATA-like* (pp_85012) were downregulated in RM tissue (Table 1). These findings are consistent with the repression of TFs related to the root vascular development process and suggest that NH_4^+ could affect PR vascular development during early exposure (Fig. 6). Nevertheless, long-term NH_4^+ nutrition promotes PR growth but causes a decrease in PR weight (Fig. 5b,c), suggesting that root radial growth could be affected by this transcriptional network.

Interestingly, in RM, the upregulation of two NAC TFs, *PpNAC31* and *PpNAC38*, similar to the *Arabidopsis SMB* and *BRN* genes (Table 1, Fig. S4), is consistent with the expression patterns of *SMB*, *BRN1* and *BRN2*, which largely overlap in *Arabidopsis* roots (Bennett *et al.*, 2010). SMB represses stem cell-like divisions in the root cap daughter cells (Bennet *et al.*, 2014; Kamiya *et al.*, 2016), and together with BRN1 and BRN2, it regulates cellular maturation of the root cap in *Arabidopsis* (Bennett *et al.*, 2010). These findings are consistent with the reduction in the number of root cap cells under NH_4^+, as described by Y. Liu *et al.*, (2013), thus providing a possible explanation for this observation in *Arabidopsis*.

In rice, the endogenous ABA content alleviates NH_4^+ rice toxicity, promoting NH_4^+ assimilation by stimulating the GS/GOGAT cycle and enhancing antioxidant activities (superoxide dismutase, ascorbate peroxidase and catalase) (Sun *et al.*, 2020). In the maritime pine root apex under NH_4^+ supply, ABA levels increased (Fig. 4d), and transcripts

encoding ABA2 enzymes (e.g. pp_198956) involved in ABA biosynthesis were upregulated in RM and RDC, and several putative ABA-induced TFs (e.g. pp_233345) were upregulated in RC and RM (Dataset S1). However, the GS/GOGAT cycle was apparently not induced, although it was observed in the whole root response to NH_4^+ supply (Ortigosa *et al.,* 2021) (Fig. 1). Regarding antioxidant metabolism, different transcripts involved in ascorbate production were downregulated (Dataset S1), including *PpBLISTER-like* TF (pp_170664) in RDC tissue (Purdy *et al.,* 2011) and two *L- gulonolactone oxidases* (pp_183087 and pp_234650) in RC and RDC tissues (Aboobucker *et al.,* 2017). This finding suggests that the glutathione-ascorbate cycle is not operative in maritime pine roots exposed to NH_4^+, which is consistent with the levels of oxidized glutathione observed under long-term experiments (Ortigosa *et al.,* 2020).

Finally, ET is involved in NH_4^+-responsive pathways in rice (Sun *et al.,* 2017) and in cambial development in poplar trees (Love *et al.,* 2009). In *Arabidopsis,* the ET levels increased under a supply of NH_4^+, which reduced lateral root formation because of the repression of auxin transporter 1 (AUX1) (Li *et al.,* 2014). In contrast, the results in maritime pine suggest a reduction in ET biosynthesis following NH_4^+ application. A transcript encoding an ACO was repressed in RM, which is consistent with proteomic and epitranscriptomic results in maritime pine whole roots (Ortigosa *et al.,* 2021). This finding is consistent with the downregulation of *BLISTER-like* TF and *L- gulonolactone oxidases* since ascorbate is one of the ACO enzyme substrates (Dilley *et al.,* 2013). Additionally, ACC was mainly located in the RM and moderately affected by NH_4^+ treatment (Fig. 4c). Accordingly, NH_4^+ stimulated the LR components (number and weight) and PR length (Fig. 5) in maritime pine, which is consistent with the increased number of root apexes under NH_4^+ nutrition compared to NO_3^- nutrition in *Pinus massoniana* Lamb. (Ren *et al.,* 2020). Taken together, the results suggest that maritime pine reduces ET biosynthesis under NH_4^+ supply, which could be linked to the PAT and CK alteration observed (Fig. 4a,b) as well as to the expression patterns observed for TFs related to cambium development (Table 1) due to the importance of IAA-ET-CK crosstalk during root development (J. Liu *et al.,* 2017).

CONCLUSIONS

NH_4^+ nutrition is a complex process in plants since NH_4^+ is a nutrient that can be toxic when supplied in excess. However, conifers in general are quite tolerant to NH_4^+. Therefore, the identifying of the differential mechanisms underlying NH_4^+ tolerance in conifers would be enormously helpful for improving NH_4^+ tolerance not only in these trees but also in other crops. In contrast to other plant models, supplying NH_4^+ to pine represses ET and ascorbate production and alters IAA and CK patterns, thus regulating a transcriptional network in the short term. Consequently, the growth and development of PR and LRs are stimulated in pine.

The expression profiles of genes related to root cambium development and phytohormones suggest a molecular mechanism underlying changes in the RSA phenotype that includes IAA-CK-ET crosstalk and a transcriptional network at least during the early root response to NH_4^+ supply. The results reported in the present study tentatively link *SHR*, and other TFs to NH_4^+ nutrition and its phenotypic effect on RSA, which likely affect early vascular development (Fig. 6).

This work provides new and valuable data to unravel the mechanisms involved in the response of maritime pine to ammonium nutrition. However, further research efforts are required to reach a full understanding of the molecular basis of ammonium tolerance.

ACKNOWLEDGEMENTS

Acknowledgments: This research was funded by Spanish *Ministerio de Economía y Competitividad*, grant numbers BIO2015-73512-JIN MINECO/AEI/FEDER, UE, RTI2018-094041-B-I00 and EQC2018-004346-P. FO was partially supported by a grant from the *Universidad de Málaga* (*Programa Operativo de Empleo Juvenil vía SNJG, UMAJI11, FEDER, FSE, Junta de Andalucía*).

Author Contributions

FO, HS and ST have performed the experiments; CLF has performed transcriptomic data analysis; FO and RAC have wrote the manuscript; CA and FMC made additional contributions and edited the manuscript; CA, FMC and RAC have acquired the funds; FO and RAC have planned and designed the research.

Conflict of Interest

The authors have no conflict of interest.

REFERENCES

Aboobucker SI, Suza WP, Lorence A. 2017. Characterization of Two *Arabidopsis* L-Gulono-1,4-lactone Oxidases, AtGulLO3 and AtGulLO5, Involved in Ascorbate Biosynthesis. *Reactive Oxygen Species (Apex)*, **4**: 389-417, doi.org/10.20455/ros.2017.861.

Antolín-Llovera M, Leivar P, Arró M, Ferrer A, Boronat A, Campos N. 2011. Modulation of plant HMG-CoA reductase by protein phosphatase 2A: positive and negative control at a key node of metabolism. *Plant Signal & Behavior* **6**:1127-31. doi: 10.4161/psb.6.8.16363.

Araya T, Kubo T, von Wirén N, Takahashi H. 2016. Statistical modeling of nitrogen-dependent modulation of root system architecture in *Arabidopsis thaliana*. *Journal of Integrative Plant Biology*, **58**: 254-265, doi.org/10.1111/jipb.12433.

Bak S, Beisson F, Bishop G, Hamberger B, Höfer R, Paquette S, Werck-Reichhart D. 2011. Cytochromes P450. The *Arabidopsis* Book/American Society of Plant Biologists, **9**, doi: 10.1199/tab.0144.

Bennett T, van den Toorn A, Sanchez-Perez GF, Campilho A, Willemsen V, Snel B, Scheres B. 2010. SOMBRERO, BEARSKIN1, and BEARSKIN2 regulate root cap maturation in *Arabidopsis*. *The Plant Cell*, **22:** 640-654, doi.org/10.1105/tpc.109.072272.

Bennett T, van den Toorn A, Willemsen V, Scheres B. 2014. Precise control of plant stem cell activity through parallel regulatory inputs. *Development*, **141**: 4055-4064, doi: 10.1242/dev.110148.

Bijlsma RJ, Lambers H, Kooijman SALM. 2000. A dynamic whole-plant model of integrated metabolism of nitrogen and carbon. 1. Comparative ecological implications of ammonium-nitrate interactions. *Plant and Soil*, **220**: 49-69.

Brady SM, Orlando DA, Lee JY, Wang JY, Koch J, Dinneny JR, Mace D, Ohler U, Benfey PN. 2007. A high-resolution root spatiotemporal map reveals dominant expression patterns. *Science*, **318:** 801-806. doi.org/10.1126/science.1146265.

Buchfink B, Xie C, Huson DH. 2015. Fast and sensitive protein alignment using DIAMOND. *Nature Methods*, **12**: 59-60, doi.org/10.1038/nmeth.3176.

Bustin SA, Benes V, Garson JA, Hellemans J, Huggett J, Kubista M, Mueller R, Nolan T, Pfaffl MW, Shipley GL et al. 2009. The MIQE guidelines: minimum information for publication of quantitative real-time PCR experiments. *Clinical Chemistry*, **55**: 611-622, doi.org/10.1373/clinchem.2008.112797.

Canales J, Flores-Monterrosso A, Rueda-López, M, Avila C and Cánovas FM. 2010. Identification of genes regulated by ammonium availability in the roots of maritime pine trees. *Amino Acids*, **39**: 991-1001. doi.org/10.1007/s00726-010-0483-9.

Canales J, Avila C, Cánovas FM. 2011. A maritime pine antimicrobial peptide involved in ammonium nutrition. *Plant Cell and Environment*, **34**: 1443-1453. doi.org/10.1111/j.1365-3040.2011.02343.x.

Canales J, Rueda-López M, Craven-Bartle B, Avila C, Cánovas FM. 2012. Novel insights into regulation of asparagine synthetase in conifers. *Frontiers in Plant Science* **3**: 100. doi.org/10.1007/s00726-010-0483-9.

Cánovas FM, Avila C, Cantón FR, Cañas RA, de la Torre F. 2007. Ammonium assimilation and amino acid metabolism in conifers. *Journal of Experimental Botany*, **58**: 2307-2318. doi.org/10.1093/jxb/erm051.

Cañas RA, de la Torre F, Cánovas FM, Cantón FR. 2006. High levels of asparagine synthetase in hypocotyls of pine seedlings suggest a role of the enzyme in re-allocation of seed-stored nitrogen. *Planta*, **224**: 83-95, doi.org/10.1007/s00425-005-0196-6.

Cañas RA, Canales J, Gómez-Maldonado J, Ávila C, Cánovas FM. 2014. Transcriptome analysis in maritime pine using laser capture microdissection and 454 pyrosequencing. *Tree Physiology*, **34**: 1278-1288, doi.org/10.1093/treephys/tpt113.

Cañas RA., Li Z, Pascual MB, Castro-Rodríguez V, Avila C, Sterck L, Van de Peer Y, Cánovas, F. M. 2017. The gene expression landscape of pine seedling tissues. *The Plant Journal*, **91**:1064-1087, doi.org/10.1111/tpj.13617.

Cao Y, Glass AD and Crawford, NM. 1993. Ammonium inhibition of *Arabidopsis* root growth can be reversed by potassium and by auxin resistance mutations aux1, axr1, and axr2. *Plant Physiology*, **102**: 983-989, doi.org/10.1104/pp.102.3.983.

Chaban C, Waller F, Furuya M, Nick P. 2003. Auxin responsiveness of a novel cytochrome p450 in rice coleoptiles. *Plant Physiology* **133**:2000-9. doi: 10.1104/pp.103.022202.

Chapman EJ, Estelle M. 2009. Mechanism of auxin-regulated gene expression in plants. *Annual Review of Genetics*, **43**: 265-285, doi.org/10.1146/annurev-genet-102108-134148.

Coll-Garcia D, Mazuch J, Altmann T, Müssig C. 2004. EXORDIUM regulates brassinosteroid-responsive genes. FEBS Letters **9**;563(1-3):82-6. doi: 10.1016/S0014-5793(04)00255-8.

Corrales AR, Carrillo L, Lasierra P, Nebauer SG, Dominguez-Figueroa J, Renau-Morata B, Pollmann S, Granell A, Molina RV, Vicente-Carbajosa J, Medina J. 2017. Multifaceted role of cycling DOF factor 3 (CDF3) in the regulation of flowering time and abiotic stress responses in Arabidopsis. *Plant, Cell & Environment*, **40**:748-764. doi: 10.1111/pce.12894.

Crook AD, Willoughby AC, Hazak O, Okuda S, VanDerMolen KR, Soyars CL, Cattaneo P, Clark NM, Sozzani R, Hothorn M, Hardtke CS, Nimchuk ZL. 2020. BAM1/2 receptor kinase signaling drives CLE peptide-mediated formative cell divisions in *Arabidopsis* roots. *Proceedings of the National Academy of Sciences, USA* **117:** 32750-32756. doi.org/10.1073/pnas.2018565117.

Cui H, Levesque MP, Vernoux T, Jung JW, Paquette AJ, Gallagher KL., Wang JY, Blilou I, Scheres B, Benfey PN. 2007. An evolutionarily conserved mechanism delimiting SHR movement defines a single layer of endodermis in plants. *Science*, **316**: 421-425, doi.org/10.1126/science.1139531.

Cui D, Zhao J, Jing Y, Fan M, Liu J, Wang Z, Xin W, Hu Y. 2013. The arabidopsis IDD14, IDD15, and IDD16 cooperatively regulate lateral organ morphogenesis and gravitropism by promoting auxin biosynthesis and transport. *PLoS Genetics* **9**,(9):e1003759. doi: 10.1371/journal.pgen.1003759.

Dilley DR, Wang Z, Kadirjan-Kalbach DK, Ververidis F, Beaudry R, Padmanabhan K. 2013. 1-Aminocyclopropane-1-carboxylic acid oxidase reaction mechanism and putative post-translational activities of the ACCO protein. *AoB Plants*, **5**: plt031, doi.org/ 10.1093/aobpla/plt031.

Domínguez-Figueroa J, Carrillo L, Renau-Morata B, Yang L, Molina RV, Marino D, Canales J, Weih M, Vicente-Carbajosa J, Nebauer SG, Medina J. 2020. The Arabidopsis Transcription Factor CDF3 Is Involved in Nitrogen Responses and Improves Nitrogen Use Efficiency in Tomato. *Frontiers in Plant Science* **11**:601558. doi: 10.3389/fpls.2020.601558.

Edgar R, Domrachev M, Lash AE. 2002. Gene Expression Omnibus: NCBI gene expression and hybridization array data repository. *Nucleic Acids Research* **30**: 207-210, doi.org/10.1093/nar/30.1.207.

Edgar RC. 2004. MUSCLE: multiple sequence alignment with high accuracy and high throughput. *Nucleic Acids Research* **32**: 1792-1797, doi.org/10.1093/nar/gkh340.

Esteban R, Ariz I, Cruz C, Moran JF. 2016. Mechanisms of ammonium toxicity and the quest for tolerance. *Plant Science*, **248**: 92-101, doi.org/10.1016/j.plantsci.2016.04.008.

Farjon A. 2018. The Kew review: conifers of the world. *Kew Bulletin*, **73**: 8, doi.org/10.1007/s12225-018-9738-5.

Felsenstein J. 1985. Confidence limits on phylogenies: An approach using the bootstrap. *Evolution*. **39**, 783-791, doi.org/10.1111/j.1558-5646.1985.tb00420.x.

Fendrych M, Van Hautegem T, Van Durme M, Olvera-Carrillo Y, Huysmans M, Karimi M, Lippens S, Guérin CJ, Krebs M, Schumacher K, Nowack MK. 2014. Programmed cell death controlled by ANAC033/SOMBRERO determines root cap organ size in Arabidopsis. *Current Biology* **24**:931-40. doi: 10.1016/j.cub.2014.03.025.

Fujita S, Ohnishi T, Watanabe B, Yokota T, Takatsuto S, Fujioka S, Yoshida S, Sakata K, Mizutani M. 2006. *Arabidopsis* CYP90B1 catalyses the early C-22 hydroxylation of C27, C28 and C29 sterols. *The Plant Journal* **45**:765-74. doi: 10.1111/j.1365-313X.2005.02639.x.

Fukaki H, Wysocka-Diller J, Kato T, Fujisawa H, Benfey PN, Tasaka M. 1998. Genetic evidence that the endodermis is essential for shoot gravitropism in *Arabidopsis thaliana*. *The Plant Journal* **14**:425-30. doi: 10.1046/j.1365-313x.1998.00137.x. PMID: 9670559.

Galinha C, Hofhuis H, Luijten M, Willemsen V, Blilou I, Heidstra R, Scheres B. 2007. PLETHORA proteins as dose-dependent master regulators of *Arabidopsis* root development. *Nature*, **449**:1053-1057, doi.org/10.1038/nature06206.

Götz S, García-Gómez JM, Terol J, Williams TD, Nagaraj SH, Nueda MJ, Robles M, Talón M, Dopazo J, Conesa A. 2008. High-throughput functional annotation and data mining with the Blast2GO suite. *Nucleic Acids Research* **36**: 3420-3435, doi.org/10.1093/nar/gkn176.

Granados JM, Avila C, Cánovas FM, Cañas RA. 2016. Selection and testing of reference genes for accurate RT-qPCR in adult needles and seedlings of maritime pine. *Tree Genetics and Genomes* **12**: 60, doi.org/10.1007/s11295-016-1018-7.

Greb T. 2020. Plant Development: How Phloem Patterning Occurs. *Current Biology*, **30**: 217-219, doi.org/10.1016/j.cub.2020.01.021.

Grunewald W, Friml J. 2010. The march of the PINs: developmental plasticity by dynamic polar targeting in plant cells. *The EMBO Journal*. **29**: 2700-2714, doi.org/10.1038/emboj.2010.181.

Guo Y, Qin G, Gu H, Qu LJ. 2009. Dof5.6/HCA2, a Dof transcription factor gene, regulates interfascicular cambium formation and vascular tissue development in *Arabidopsis*. *The Plant Cell* **21**(11):3518-34. doi: 10.1105/tpc.108.064139.

Haas BJ, Papanicolaou A, Yassour M, Grabherr M, Blood PD, Bowden J, Couger MB, Eccles D, Li B, Lieber M, MacManes MD, Ott M, Orvis J, Pochet N, Strozzi F, Weeks N, Westerman R, William T, Dewey CN, Henschel R, LeDuc RD, Friedman N, Regev A. 2013. *De novo* transcript sequence reconstruction from RNA-seq using the Trinity platform for reference generation and analysis. *Nature Protocols*, **8**: 1494-1512, doi: 10.1038/nprot.2013.084.

Hachiya T, Sakakibara H. 2017. Interactions between nitrate and ammonium in their uptake, allocation, assimilation, and signaling in plants. *Journal of Experimental Botany*, **68**: 2501-2512, doi.org/10.1093/jxb/erw449.

Hawkins BJ, Robbins S. 2010. pH affects ammonium, nitrate and proton fluxes in the apical region of conifer and soybean roots. *Physiologia Plantarum*, **138**: 238-247, doi.org/10.1111/j.1399-3054.2009.01317.x.

Helariutta Y, Fukaki,H, Wysocka-Diller J, Nakajima K, Jung J, Sena G, Hauser MT, Benfey PN. 2000. The SHORT-ROOT gene controls radial patterning of the Arabidopsis root through radial signaling. *Cell*, **101**: 555-567, doi.org/10.1016/S0092-8674(00)80865-X.

Hong ZH, Qing T, Schubert D, Kleinmanns JA, Liu JX. 2019. BLISTER-regulated vegetative growth is dependent on the protein kinase domain of ER stress modulator IRE1A in *Arabidopsis thaliana*. *PLoS Genetics* **15**:e1008563. doi: 10.1371/journal.pgen.1008563. PMID: 31869326; PMCID: PMC6946172.

Hou H, Erickson J, Meservy J, Schultz EA. 2010. FORKED1 encodes a PH domain protein that is required for PIN1 localization in developing leaf veins. *The Plant Journal*, **63**: 960-973, doi.org/10.1111/j.1365-313X.2010.04291.x.

Houben M, Van de Poel B. 2019. 1-Aminocyclopropane-1-Carboxylic Acid Oxidase (ACO): The Enzyme That Makes the Plant Hormone Ethylene. Frontiers in Plant Science **10**:695. doi: 10.3389/fpls.2019.00695.

Kamada-Nobusada T, Makita N, Kojima M, Sakakibara H. 2013. Nitrogen-dependent regulation of de novo cytokinin biosynthesis in rice: the role of glutamine metabolism as an additional signal. *Plant and Cell Physiology*, **54**: 1881-1893, doi.org/10.1093/pcp/pct127.

Kamiya M, Higashio SY, Isomoto A, Kim JM, Seki M, Miyashima S, Nakajima K. 2016. Control of root cap maturation and cell detachment by BEARSKIN transcription factors in *Arabidopsis*. *Development*, **143**: 4063-4072, doi: 10.1242/dev.142331.

Kim H, Zhou J, Kumar D, Jang G, Ryu KH, Sebastian J, Miyashima S, Helariutta Y, Lee JY. 2020. SHORTROOT-Mediated Intercellular Signals Coordinate Phloem Development in *Arabidopsis* Roots. *The Plant Cell*, **32**; 1519-1535, doi.org/10.1105/tpc.19.00455.

Kronzucker HJ, Siddiqi MY, Glass AD. 1997. Conifer root discrimination against soil nitrate and the ecology of forest succession. *Nature*, **385**; 59-61, doi.org/10.1038/385059a0.

Kumar S, Stecher G, Tamura K. 2016. MEGA7: Molecular Evolutionary Genetics Analysis version 7.0 for bigger datasets. *Molecular Biology and Evolution*, **33**: 1870-1874, doi.org/10.1093/molbev/msw054.

Kuroha T, Tokunaga H, Kojima M, Ueda N, Ishida T, Nagawa S, Fukuda H, Sugimoto K, Sakakibara H. 2009. Functional analyses of LONELY GUY cytokinin-activating enzymes reveal the importance of the direct activation pathway in *Arabidopsis*. *The Plant Cell*, **21**: 3152-3169, doi.org/10.1105/tpc.109.068676.

Liao Z, Chen M, Guo L, Gong Y, Tang F, Sun X, Tang K. 2004. Rapid isolation of high-quality total RNA from taxus and ginkgo. *Preparative Biochemistry & Biotechnology* **34**: 209-214, doi.org/10.1081/PB-200026790.

Lima JE, Kojima S, Takahashi H, von Wirén N. 2010. Ammonium triggers lateral root branching in *Arabidopsis* in an AMMONIUM TRANSPORTER1;3-dependent manner. *Plant Cell*, **22**: 3621– 3633, doi.org/10.1105/tpc.110.076216.

Liu Y, Lai N, Gao K, Chen F, Yuan L, Mi G. 2013. Ammonium inhibits primary root growth by reducing the length of meristem and elongation zone and decreasing elemental expansion rate in the root apex in *Arabidopsis thaliana*. *PLoS One*, **8:** e61031, doi.org/10.1371/journal.pone.0061031.

Liu Y, von Wirén N. 2017. Ammonium as a signal for physiological and morphological responses in plants. *Journal of Experimental Botany*, **68**: 2581-2592, doi.org/10.1093/jxb/erx086.

Love J, Björklund S, Vahala J, Hertzberg M, Kangasjärvi J, Sundberg B. 2009. Ethylene is an endogenous stimulator of cell division in the cambial meristem of *Populus*. *Proceedings of the National Academy of Sciences, USA* **106**: 5984-5989. doi.org/10.1073/pnas.0811660106.

Lucas M, Swarup R, Paponov IA, Swarup K, Casimiro I, Lake D, Peret B, Zappala S, Mairhofer S, Whitworth M, Wang J, Ljung K, Marchant A, Sandberg G, Holdsworth MJ, Palme K, Pridmore T, Mooney S, Bennett MJ. 2011. Short-Root regulates primary, lateral, and adventitious root development in *Arabidopsis*. *Plant Physiology* **155**: 384-398. doi.org/10.1104/pp.110.165126.

Mao C, He J, Liu L, Deng Q, Yao X, Liu C, Qiao Y, Li P, Ming F. 2020. OsNAC2 integrates auxin and cytokinin pathways to modulate rice root development. *Plant Biotechnology Journal*, **18**: 429-442, doi.org/10.1111/pbi.13209.

Marhava P, Bassukas AEL, Zourelidou M, Kolb M, Moret B, Fastner A, Schulze WX, Cattaneo P, Hammes UZ, Schwechheimer C, Hardtke CS. 2018. A molecular rheostat adjusts auxin flux to promote root protophloem differentiation. *Nature*, **558:** 297-300, doi.org/10.1038/s41586-018-0186-z

Men S, Boutté Y, Ikeda Y, Li X, Palme K, Stierhof YD, Hartmann MA, Moritz T, Grebe M. 2008. Sterol-dependent endocytosis mediates post-cytokinetic acquisition of PIN2 auxin efflux carrier polarity. *Nature Cell Biology*, **10**: 237-244, doi.org/10.1038/ncb1686.

Miller AJ, Cramer MD. 2005. Root nitrogen acquisition and assimilation. In Root physiology: From gene to function. *Springer*, Dordrecht, 1-36, doi.org/10.1007/1-4020-4099-7_1.

Miyashima S, Koi S, Hashimoto T, Nakajima K. 2011. Non-cell-autonomous microRNA165 acts in a dose-dependent manner to regulate multiple differentiation status in the *Arabidopsis* root. *Development*, **138**:2303-2313, doi: 10.1242/dev.060491.

Miyashima S, Roszak P, Sevilem I, Toyokura K, Blob B, Heo, JO, Mellor N, Rinta-Rahko HH, Otero S, et al. 2019. Mobile PEAR transcription factors integrate positional cues to prime cambial growth. *Nature*, **565**: 490-494, doi.org/10.1038/s41586-018-0839-y.

Moreno-Risueno MA, Martínez M, Vicente-Carbajosa J, Carbonero P. 2007. The family of DOF transcription factors: from green unicellular algae to vascular plants. *Molecular Genetics and Genomics* **277**: 379-90, doi.org/10.1007/s00438-006-0186-9.

Moritake S, Taira S, Ichiyanagi Y, Morone N, Song SY, Hatanaka T, Yuasa S, Setou M. 2007. Functionalized nano-magnetic particles for an *in vivo* delivery system. *Journal of Nanoscience and Nanotechnology*, **7**: 937-944, doi.org/10.1166/jnn.2007.216.

Nakajima K, Sena G, Nawy T, Benfey, PN. 2001. Intercellular movement of the putative transcription factor SHR in root patterning. *Nature* **413**: 307–311, doi.org/10.1038/35095061.

Näsholm T, Ekblad A, Nordin A, Giesler R, Högberg M, Högberg P. 1998. Boreal forest plants take up organic nitrogen. *Nature*, **392**: 914-916, doi.org/10.1038/31921.

NCBI Resource Coordinators. 2016. Database resources of the National Center for Biotechnology Information. *Nucleic Acids Research* **44**: 7-19.

Ochando I, Jover-Gil S, Ripoll JJ, Candela H, Vera A, Ponce MR, Martínez-Laborda A, Micol JL. 2006. Mutations in the microRNA complementarity site of the INCURVATA4 gene perturb meristem function and adaxialize lateral organs in *Arabidopsis*. *Plant Physiology* **141**: 607-619, doi.org/10.1104/pp.106.077149.

Ortigosa F, Valderrama-Martín JM, Urbano-Gámez JA, García-Martín ML, Ávila C, Cánovas FM, Cañas RA. 2020. Inorganic nitrogen form determines nutrient allocation and metabolic responses in maritime pine seedlings. *Plants*, **9**: 481, doi.org/10.3390/plants9040481.

Ortigosa F, Lobato-Fernández C, Pérez-Claros JA, Cantón FR, Ávila C, Cánovas FM, Cañas RA. 2021. Epitranscriptome changes triggered by ammonium nutrition regulate the proteome response of maritime pine roots. *bioRxiv*. doi.org/10.1101/2021.04.20.440618.

Patterson K, Cakmak T, Cooper A, Lager IDA, Rasmusson AG, Escobar MA. 2010. Distinct signalling pathways and transcriptome response signatures differentiate

ammonium-and nitrate-supplied plants. *Plant, Cell & Environment*, **33**: 1486-1501, doi.org/10.1111/j.1365-3040.2010.02158.x.

Prigge MJ, Otsuga D, Alonso J M, Ecker JR, Drews GN, Clark, SE. 2005. Class III homeodomain-leucine zipper gene family members have overlapping, antagonistic, and distinct roles in *Arabidopsis* development. *The Plant Cell*, **17**:61-76, doi.org/10.1105/tpc.104.026161.

Purdy SJ, Bussell JD, Nelson DC, Villadsen D, Smith SM. 2011. A nuclear-localized protein, KOLD SENSITIV-1, affects the expression of cold-responsive genes during prolonged chilling in *Arabidopsis*. *Journal of Plant Physiology*, **168**: 263-269, doi.org/10.1016/j.jplph.2010.07.001.

Ravazzolo L, Trevisan S, Forestan C, Varotto S, Sut S, Dall'Acqua S, Malagoli M, Quaggiotti S. (2020). Nitrate and ammonium affect the overall maize response to nitrogen availability by triggering specific and common transcriptional signatures in roots. *International Journal of Molecular Sciences*, **21**: 686, doi.org/10.3390/ijms21020686.

Ren Q, Zhou Y, Zhou X. 2020. Combined Transcriptome and Proteome Analysis of Masson Pine (*Pinus massoniana* Lamb.) Seedling Root in Response to Nitrate and Ammonium Supplementations. *International Journal of Molecular Sciences*, **21**: 7548, doi.org/10.3390/ijms21207548.

Ritz C, Spiess AN. 2008. qpcR: an R package for sigmoidal model selection in quantitative real-time polymerase chain reaction analysis. *Bioinformatics* **24**: 1549-1551, doi.org/10.1093/bioinformatics/btn227.

Roodbarkelari F, Groot EP. 2017. Regulatory function of homeodomain-leucine zipper (HD-ZIP) family proteins during embryogenesis. *New Phytologist*, **213**: 95-104, doi.org/10.1111/nph.14132.

Rubio V, Linhares F, Solano R, Martín AC, Iglesias J, Leyva A, Paz-Ares J. 2001. A conserved MYB transcription factor involved in phosphate starvation signaling both in vascular plants and in unicellular algae. *Genes & Development* **15**(16):2122-33. doi: 10.1101/gad.204401.

Sablowski R. 2011. Plant stem cell niches: from signalling to execution. *Current Opinion in Plant Biology*, **14**: 4-9, doi.org/10.1016/j.pbi.2010.08.001.

Saitou N, Nei M. 1987. The neighbor-joining method: A new method for reconstructing phylogenetic trees. *Molecular Biology and Evolution* **4**: 406-425, doi.org/10.1093/oxfordjournals.molbev.a040454.

Schatlowski N, Stahl Y, Hohenstatt ML, Goodrich J, Schubert D. 2010. The CURLY LEAF interacting protein BLISTER controls expression of polycomb-group target genes and cellular differentiation of *Arabidopsis thaliana*. *The Plant Cell* **22**:2291-305. doi: 10.1105/tpc.109.073403.

Schoenbohm C, Martens S, Eder C, Forkmann G, Weisshaar B. 2000. Identification of the *Arabidopsis thaliana* flavonoid 3'-hydroxylase gene and functional expression of the encoded P450 enzyme. *Biological Chemistry* **381**:749-53. doi: 10.1515/BC.2000.095.

Schwarz R, Dayhoff M. 1979. Matrices for detecting distant relationships. In Dayhoff M., editor, *Atlas of protein sequences*:353-58. *National Biomedical Research Foundation*.

Sena G, Jung, JW, Benfey PN. 2004. A broad competence to respond to SHORT ROOT revealed by tissue-specific ectopic expression. *Development* **131**: 2817–2826, doi: 10.1242/dev.01144.

Shiono K, Taira S. 2020. Imaging of Multiple Plant Hormones in Roots of Rice (Oryza sativa) Using Nanoparticle-Assisted Laser Desorption/Ionization Mass Spectrometry. *Journal of Agricultural and Food Chemistry* **68**: 6770-6775. doi: 10.1021/acs.jafc.0c00749.

Shtratnikova VY, Kudryakova NV, Kudoyarova GR, Korobova AV, Akhiyarova GR, Danilova MN, Kustetsov VV, Kulaeva ON. 2015. Effects of nitrate and ammonium on growth of *Arabidopsis thaliana* plants transformed with the ARR5::GUS construct and a role for cytokinins in suppression of disturbances induced by the presence of ammonium. *Russian Journal of Plant Physiology*, **62**: 741-752, doi.org/10.1134/S1021443715060151.

Smit ME, Llavata-Peris CI, Roosjen M, van Beijnum H, Novikova D, Levitsky V, Sevilem I, Roszak P, Slane D, Jürgens G, Mironova V, Brady SM, Weijers D. 2020. Specification and regulation of vascular tissue identity in the *Arabidopsis* embryo. *Development* **147**(8):dev186130. doi: 10.1242/dev.186130. PMID: 32198154.

Sun L, Di D, Li G, Kronzucker HJ, Shi W. 2017. Spatio-temporal dynamics in global rice gene expression (*Oryza sativa* L.) in response to high ammonium stress. *Journal of Plant Physiology*, **212**: 94-104. doi.org/10.1016/j.jplph.2017.02.006.

Sun L, Di DW, Li G, Kronzucker HJ, Wu X, Shi W. 2020. Endogenous ABA alleviates rice ammonium toxicity by reducing ROS and free ammonium via regulation of the SAPK9–bZIP20 pathway. *Journal of Experimental Botany*, **71**: 4562–4577, doi.org/10.1093/jxb/eraa076.

Supek F, Bošnjak M, Škunca N, Šmuc T. 2011. REVIGO summarizes and visualizes long lists of gene ontology terms. *PLoS One*, **6**:e21800. doi: 10.1371/journal.pone.0021800.

Takei K, Ueda N, Aoki K, Kuromori T, Hirayama T, Shinozaki K, Yamaya T, Sakakibara H. 2004. AtIPT3 is a key determinant of nitrate-dependent cytokinin biosynthesis in *Arabidopsis*. *Plant and Cell Physiology*, ***45***: 1053-1062, doi.org/10.1093/pcp/pch119.

Tan W, Zhang D, Zhou H, Zheng T, Yin Y, Lin H. 2018. Transcription factor HAT1 is a substrate of SnRK2.3 kinase and negatively regulates ABA synthesis and signaling in *Arabidopsis* responding to drought. *PLoS Genetics* **14**:e1007336. doi: 10.1371/journal.pgen.1007336.

Tian Tian, Yue Liu, Hengyu Yan, Qi You, Xin Yi, Zhou Du, Wenying Xu, Zhen Su. 2017. agriGO v2.0: a GO analysis toolkit for the agricultural community. *Nucleic Acids Research* **45**: 122-129, doi.org/10.1093/nar/gkx382.

Wang S, Chang Y, Guo J, Zeng Q, Ellis BE, Chen JG. 2011. *Arabidopsis* ovate family proteins, a novel transcriptional repressor family, control multiple aspects of plant growth and development. *PLoS One* **6**:e23896. doi: 10.1371/journal.pone.0023896.

Ward JM, Cufr CA, Denzel MA, Neff MM. 2005. The Dof transcription factor OBP3 modulates phytochrome and cryptochrome signaling in *Arabidopsis*. *The Plant Cell* **17**:475-85. doi: 10.1105/tpc.104.027722.

Warren CR, Adams MA. 2002. Possible causes of slow growth of nitrate-supplied *Pinus pinaster*. *Canadian Journal of Forest Research*, **32**:569-580, doi.org/10.1139/x01-225.

Werner T, Motyka V, Laucou V, Smets R, Van Onckelen H, Schmülling T. 2003. Cytokinin-deficient transgenic *Arabidopsis* plants show multiple developmental alterations indicating opposite functions of cytokinins in the regulation of shoot and root meristem activity. *The Plant Cell*, **15**: 2532-2550, doi.org/10.1105/tpc.014928.

Willemsen V, Bauch M, Bennett T, Campilho A, Wolkenfelt H, Xu J, Haseloff J, Scheres B. 2008. The NAC domain transcription factors FEZ and SOMBRERO control the

orientation of cell division plane in Arabidopsis root stem cells. *Developmental Cell* **15**:913-22. doi: 10.1016/j.devcel.2008.09.019.

Xu J, Hofhuis H, Heidstra R, Sauer M, Friml J, Scheres B. 2006. A molecular framework for plant regeneration. *Science*, **311**: 385-388, doi.org/10.1126/science.1121790.

Youssef C, Bizet F, Bastien R, Legland D, Bogeat-Triboulot MB, Hummel I. 2018. Quantitative dissection of variations in root growth rate: a matter of cell proliferation or of cell expansion?, *Journal of Experimental Botany*, **69**: 5157–5168, doi.org/10.1093/jxb/ery272.

Zhang D, Ye H, Guo H, Johnson A, Zhang M, Lin H, Yin Y. 2014. Transcription factor HAT1 is phosphorylated by BIN2 kinase and mediates brassinosteroid repressed gene expression in *Arabidopsis*. *The Plant Journal* **77**: 59-70. doi: 10.1111/tpj.12368.

Zhang S, Wang X. 2017. One new kind of phytohormonal signaling integrator: Up-and-coming GASA family genes. *Plant Signal & Behavior* **12**:e1226453. doi: 10.1080/15592324.2016.1226453.

Zhang W, Swarup R, Bennett M, Schaller GE, Kieber JJ. 2013. Cytokinin induces cell division in the quiescent center of the *Arabidopsis* root apical meristem. *Current Biology*, **23:** 1979-1989. doi.org/10.1016/j.cub.2013.08.008.

Zhou W, Wei L, Xu J, Zhai Q, Jiang, H, Chen R, Chen Q, Sun J, Chu J Zhu Let al. 2010. *Arabidopsis* tyrosylprotein sulfotransferase acts in the auxin/PLETHORA pathway in regulating postembryonic maintenance of the root stem cell niche. *The Plant Cell*, **22**: 3692-3709, doi.org/10.1105/tpc.110.075721.

Zou N, Li B, Chen H, Su Y, Kronzucker HJ, Xiong L, Baluška F, Shi W. 2013. GSA-1/ARG 1 protects root gravitropism in *Arabidopsis* under ammonium stress. New Phytologist, **200**: 97-111, doi.org/10.1111/nph.12365.

Zúñiga-Mayo VM, Marsch-Martínez N, de Folter S. 2012. The class II HD-ZIP JAIBA gene is involved in meristematic activity and important for gynoecium and fruit development in *Arabidopsis*. *Plant Signal & Behavior* **7**: 1501-3. doi: 10.4161/psb.21901.

959 **Table 1.** Most representative DE transcripts coding for TFs and hormone related proteins.

TF in maritime pine	Gene ID	Tissue	Transcript in *A.thaliana*	Gene ID	Process involved	References
PpDOF11	*pp_58878*	RC	*HCA2/ DOF5.6*	*AT5G62940*	Root tip vascular proliferation: radial growth of protophloem sieve elements	Guo *et al.*, 2009 Miyashima *et al.*,2019
PpSHR	*pp_246622*	RC	*SHR*	*AT4G37650*	- Quiescent center cells specification - Asymmetric cell division related to rootradial pattern formation - Phloem development	Fukaki *et al.*, 1998 Helariutta *et al.*, 2000 Cui *et al.*, 2007 Kim *et al.*, 2020
PpGATA20-like	*pp_204819*	RC	*GATA20*	*AT2G18380*	Root tip vascular development	Smit *et al.*, 2020
PpSGR/IDD 16	*pp_174625*	RC	*IDD14*	*AT1G68130*	- Lateral organ morphogenesis and gravitropic responses - Establishment of auxin gradients (auxin biosynthesis and transport)	Cui *et al.*, 2013
PpPHR1-like	*pp_64350*	RD C	*PHR1*	*AT4G28610*	Phosphate starvation	Rubio *et al.*, 2001
PpOFP17	*pp_80824*	RD C	*OFP17*	*AT2G30395*	Plant growth and development	Wang *et al.*, 2011
PpBLISTER-like	*pp_170664*	RD C	*BLISTER*	*AT3G23980*	Plant vegetative growth	Schatlowski*et al.*, 2010 Hong *et al.*, 2019

PpDOF2	*pp_119525*	RD C	*PEAR1/ DOF2.4*	*AT2G37590*	Root tip vascular proliferation: radial growth ofprotophloem sieve elements	Miyashima *et al.*,2019
PpDOF12	*pp_85381*	RM	*CDF3*	*AT3G47500*	Involved in abiotic stress tolerance and nitrogen response	Corrales *et al.*, 2017 Domínguez-Figueroa*et al.*, 2020
PpDOF1	*pp_233816*	RM	*OPB3*	*AT3G55370*	Regulator of phyB and cry1 signaling pathways	Ward *et al.*, 2005
PpHAT-like	*pp_141831*	RM	*HAT1*	*AT4G1746 0*	- Inflorescence meristem regulation, floralmeristem determination, gynoecium medial domain development - Repressor of BR responsive genes and ABA biosynthesis	Zúñiga-Mayo *et al.*, 2012 Zhang *et al.*, 2014 Tan *et al.*, 2018
PpINCURV ATA-like	*pp_85012*	RM	*ATBH-15*	*AT1G52150*	Root meristem patterning and putatively in the regulation of procambial and vascular tissue formation or maintenance.	Ochando *et al.*, 2006
PpNAC31	*pp_168080*	RM	*SMB*	*AT1G79580*	Cellular maturation of root cap regulation	Willemsen *et al.*, 2008 Bennett *et al.*, 2010 Fendrych *et al.*, 2014
PpNAC38	*pp_72282*	RM	*BRN1/BRN2*	*AT1G33280*	Cellular maturation of root cap regulation	Bennett *et al.*, 2010
PpVAN3/FKD2	*pp_60103*	RC and RM	*VAN3/ FORKED2*	*AT5G13300*	Plant vascular tissue formation by PIN transporters localization	Steynen and Schultz, 2003 Naramoto *et al.*, 2009 Hou *et al.*, 2010
Cytokinin riboside 5'-monophosphate phosphoribohydrol ase	*pp_222714*	RC	*LOG3*	*AT2G37210*	Cytokinin activation	Kuroha *et al.*, 2009

Cycloeucalenol cycloisomerase	*pp_189071*	RC	*CPII*	*AT5G50375*	PIN2 endocytosis	Men *et al.*, 2008
Sulfotransferase	*pp_208269*	RDC	*SULT20B1*	*AT3G45070*	Flavonoids sulfation	Hashiguchi *et al.*, 2013
PpABA2	*pp_198945*	RDC and RM	*ABA2*	*AT1G52340*	Biosynthesis of abscisic acid	González-Guzmán *et al.*, 2002
PpCYP90B1	*pp_247190*	RDC	*CYP90B1*	*AT3G50660*	Biosynthesis of brassinosteroids	Fujita *et al.*, 2006
PpTIR1	*pp_238715*	RDC	*TIR1*	*AT3G62980*	Auxin signalling pathway	Dharmasiri *et al.*, 2005 Salehin *et al.*, 2015
PpCYP87A3	*pp_81114*	RDC	*CYP87A2*	*AT1G12740*	Putatively involved in hormone biosynthesis and/or auxin signaling	Chaban *et al.*, 2003 Bark *et al.*, 2011
GASA gibberellin regulated cysteine richprotein	*pp_111379*	RDC	*GASA10*	*AT5G59845*	Putatively involved in response tophytohormones	Zhang and Wang, 2017
HMG-CoA reductase	*pp_144669*	RDC	*HMGR*	*AT2G17370*	Regulatory enzyme of the cytokinin and brassinosteroid biosynthesis pathways	Antolín-Llovera et al., 2011
PpABA2	*pp_209084*	RDC	*ABA2*	*AT1G52340*	Biosynthesis of abscisic acid	González-Guzmán *etal.*, 2002

Cytokinin dehydrogenase	*pp_215376*	RDC	*CKX1*	*AT2G41510*	Catalyzes the oxidation of cytokinins	Werner *et al.*, 2003
PpACO	*pp_202153*	RM	*ACO*	*AT2G19590*	Ethylene biosynthesis	Houben *et al.*, 2019
Flavonoid 3'-monooxygenase	*pp_203885*	RM	*F3'H*	*AT5G07990*	Involved in flavonoids biosynthesispathway from naringenin to eriodictyol and dihydrokaempferol to dihydroquercetin	Schoenbohm et al., 2000
EXORDIUM	*pp_129078*	RM	*EXO*	*AT4G08950*	Putatively involved in brassinosteroids resopnse in roots	Coll-Garcia et al., 2004

Figure legends

Fig. 1. Experimental design. Timeline from germination to harvest. RT-qPCR data for the validation of the experimental design are included. *Glutamine synthetase 1b* (*PpGS1b*); *NADH-dependent glutamate synthase* (*PpNADH-GOGAT*); *antimicrobial peptide 1* (*PpAMP1*); *S-adenosyl methionine synthase* (*PpSAMS*) Significant differences were determined with a *t*-test (* *P*-value < 0.05; ** *P*-value < 0.01). Error bars show SE with n = 3.

Fig. 2. Low-input RNA-seq results in the different tissues of maritime pine root tip. (**a**) Venn diagram of down-regulated DE transcripts. (**b**) Venn diagram of up-regulated DE transcripts. (**c**) Heatmap and hierarchical clustering of DE transcripts. Expression values correspond to median CPM between biological/experimental replicates. The hierarchical clustering was made employing the Ward's minimum variance method. (**d**) Experimental validation of low-input RNA-seq results for 8 DE transcripts through RT-qPCR. RC, the root cap; RM, root meristem; RDC, root developing cortex; and RDV, root developing vessels. *SHORT-ROOT* (*PpSHR*); *nitrate transporter 1 / peptide transporter family 3.1* (*PpNPF3.1*); *cycloeucalenol cycloisomerase* (*PpCPI1*); *DOF transcription factor 12* (*PpDOF12*); *NAC transcription factor 38* (*PpNAC38*); *aminocyclopropane-1-carboxylic acid oxidase* (*PpACO*); *antimicrobial peptide 1* (*PpAMP1*); *BLISTER-like transcription factor* (*PpBLISTER-like*).

Fig. 3. Resume of the main functional results obtained in the low-input RNA-Seq analysis from LCM isolated samples. Functions and DE transcripts in (**a**) the root cap (RC), (**b**) root meristem (RM), (**c**) root developing cortex (RDC) and (**d**) root developing vessels (RDV). Blue arrows indicate downregulated transcripts, red arrows upregulated ones. (**e**) Significant GO terms from Biological Processes category after a SEA analysis. (**f**) Significant GO terms from Molecular Function category after a SEA analysis.

Fig. 4. Phytohormone localization in root apex sections. The main phytohormones were localized in root apex cuts of control and 3 mM NH_4^+ treated seedlings. The phytohormone identification and imaging was made using nano-particle assisted laser

desorption/ionization mass spectrometry imaging (Nano-PALDI-MSI). (**a**) Auxin / Indole-3-acetic acid (IAA); (**b**) cytokinin (CK); (**c**) aminocyclopropane-1-carboxylic acid (ACC); (**d**) abscisic acid (ABA). Size bars correspond to 500 µm.

Fig. 5. Root growth and architecture parameters. Pine seedlings were cultivated for 74 days and irrigated once a week with 50 mL of water, 3 mM KNO_3 and 3 mM NH_4Cl, respectively. Six different parameters were measured after harvesting: (**a**) weight of whole roots; (**b**) weight of primary root; (**c**) primary root length; (**d**) number of lateral roots; (**e**) weight of lateral roots; (**f**) lateral root density. Significant differences were determined with a one-way ANOVA. Letters above the conditions show significant differences based on a Turkey post-hoc test ($P < 0.05$) with a n = 30.

Fig. 6. Schematic representation of the transcriptional response induced by NH_4^+ supply in maritime pine seedling roots 24 h after irrigation. Transcripts in red letters are upregulated. Transcripts in blue letters are downregulated. The root tip tissues are the root cap (RC) root meristem (RM) and root developing cortex (RDC). Results for root developing vessels (RDV) are not shown since they were very limited.

Supporting information

Video S1. LCM cutting procedure.

Table S1. LCM low-input RNA sequencing results.

Table S2. List of used primers.

Table S3. Protein sequences of DOF transcription factors in maritime pine, *Arabidopsis* and rice.

Table S4. Protein sequences of NAC transcription factors in maritime pine and *Arabidopsis*.

Method S1. Complete LCM and cDNA amplification procedures.

Fig. S1. Aspect of root architecture after long-term nutritional treatments.

Fig. S2. MDS plot of the LCM low-input RNA-seq samples.

Fig. S3. Phylogenetic tree of DOF transcription factor family in maritime pine, *Arabidopsis* and rice. The protein sequences employed to infer the phylogenetic tree are presented in the Table S3. The protein sequence alignment was made with Muscle (Edgar, 2004). The evolutionary history was inferred using the Neighbor-Joining method (Saitou and Nei, 1987). The bootstrap consensus tree inferred from 1000 replicates is taken to represent the evolutionary history of the taxa analyzed (Felsenstein, 1985). Branches corresponding to partitions reproduced in less than 50% bootstrap replicates are collapsed. The evolutionary distances were computed using the Dayhoff matrix-based method (Schwarz and Dayhoff, 1979) and are in the units of the number of amino acid substitutions per site. The analysis involved 78 amino acid sequences. All positions containing gaps and missing data were eliminated. There were 54 positions in the final dataset mainly corresponding to the DOF domain. Evolutionary analyses were conducted in MEGA7 (Kumar *et al.*, 2016). DOFs from maritime pine have a red dot and their names are in bold. Abbreviations: At, *Arabidopsis thaliana*; Pp, *Pinus pinaster*; Os, *Oryza sativa*.

Fig. S4. Phylogenetic tree of NAC transcription factor family in maritime pine and *Arabidopsis*. The protein sequences employed to infer the phylogenetic tree are presented in the Table S4. The protein sequence alignment was made with Muscle (Edgar, 2004). The evolutionary history was inferred using the Neighbor-Joining method (Saitou and Nei, 1987). The bootstrap consensus tree inferred from 1000 replicates is taken to represent the evolutionary history of the taxa analyzed (Felsenstein, 1985). Branches corresponding to partitions reproduced in less than 50% bootstrap replicates are collapsed. The evolutionary

distances were computed using the Dayhoff matrix-based method (Schwarz and Dayhoff, 1979) and are in the units of the number of amino acid substitutions per site. The analysis involved 151 amino acid sequences. All positions with less than 80% site coverage were eliminated. That is, fewer than 20% alignment gaps, missing data, and ambiguous bases were allowed at any position. There were 261 positions in the final dataset. Evolutionary analyses were conducted in MEGA7 (Kumar *et al.*, 2016). NACs from maritime pine have a red dot and their names are in bold.

Fig. S5. Salicylic acid and jasmonic acid localization in root tip sections. The phytohormones were localized in root apex cuts of control and 3 mM NH_4^+ treated seedlings. The phytohormone identification and imaging was made using nano-particle assisted laser desorption/ionization mass spectrometry imaging (Nano-PALDI-MSI). (**a**) Salicylic acid (SA); (**b**) jasmonic acid (JA). Size bars correspond to 500 µm.

Fig. S6. Expression atlas of *PpDof1* in the tissues of one-month old seedlings (Cañas *et al.*, 2017).

Fig. S7. Expression atlas of *PpDof2* in the tissues of one-month old seedlings (Cañas *et al.*, 2017).

Fig. S8. Expression atlas of *PpDof11* in the tissues of one-month old seedlings (Cañas *et al.*, 2017).

Fig. S9. Expression atlas of *PpDof12* in the tissues of one-month old seedlings (Cañas *et al.*, 2017).

Dataset S1. LCM low-input RNA-seq differential expression results. DE transcripts up-regulated are in highlighted red. DE transcripts down-regulated are in highlighted blue.

Dataset S2. LCM low-input RNA-seq clustering results of DE transcripts.

Dataset S3. LCM low-input RNA-seq functional enrichment of DE transcripts. Only conditions with significant functions are shown.

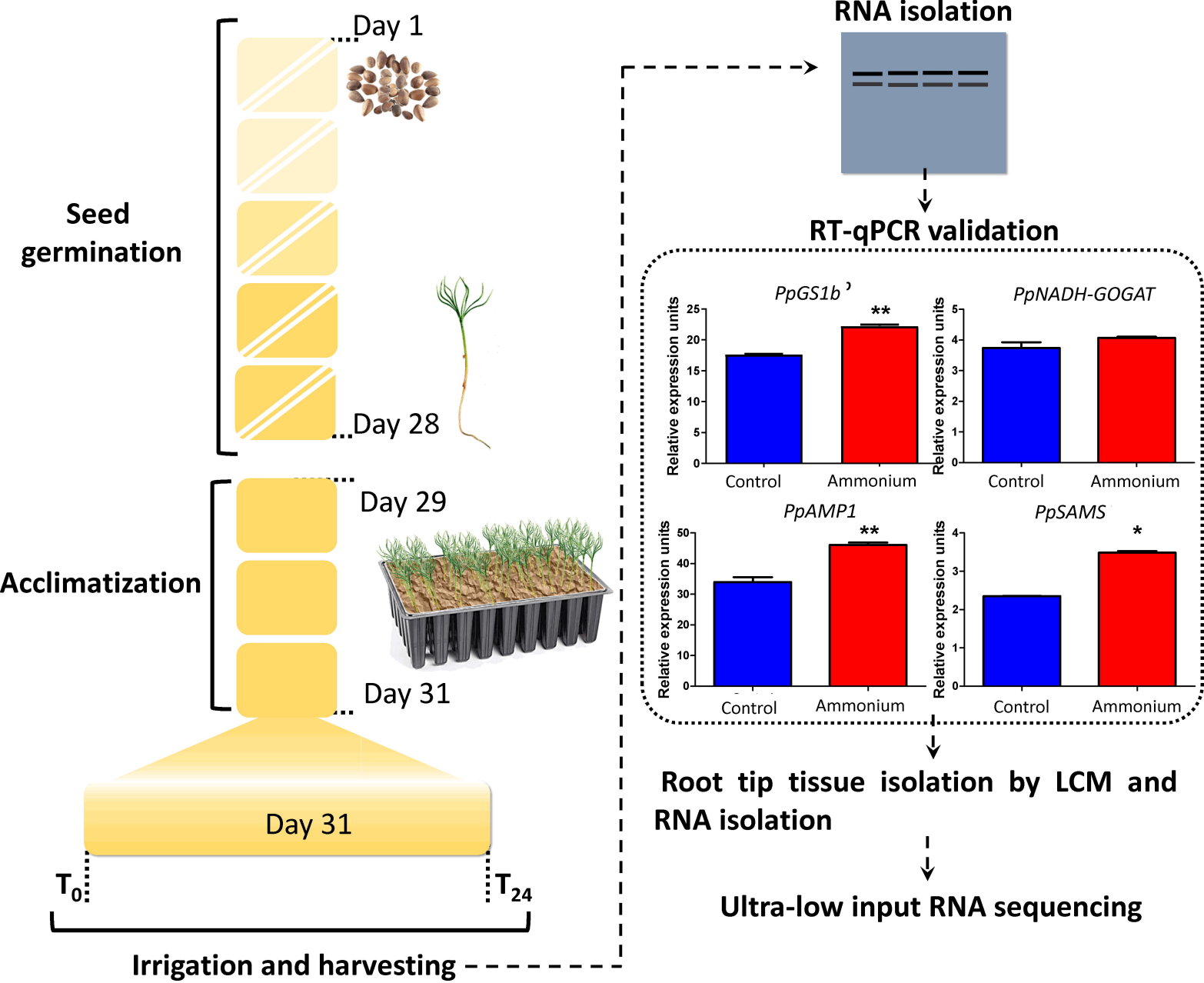

Fig. 1. Experimental design. Timeline from germination to harvest. RT-qPCR data for the validation of the experimental design are included. *Glutamine synthetase 1b* (*PpGS1b*); *NADH-dependent glutamate synthase* (*PpNADH-GOGAT*); *antimicrobial peptide 1* (*PpAMP1*); *S-adenosyl methionine synthase* (*PpSAMS*) Significant differences were determined with a *t*-test (* P-value < 0.05; ** P-value < 0.01). Error bars show SE with n = 3.

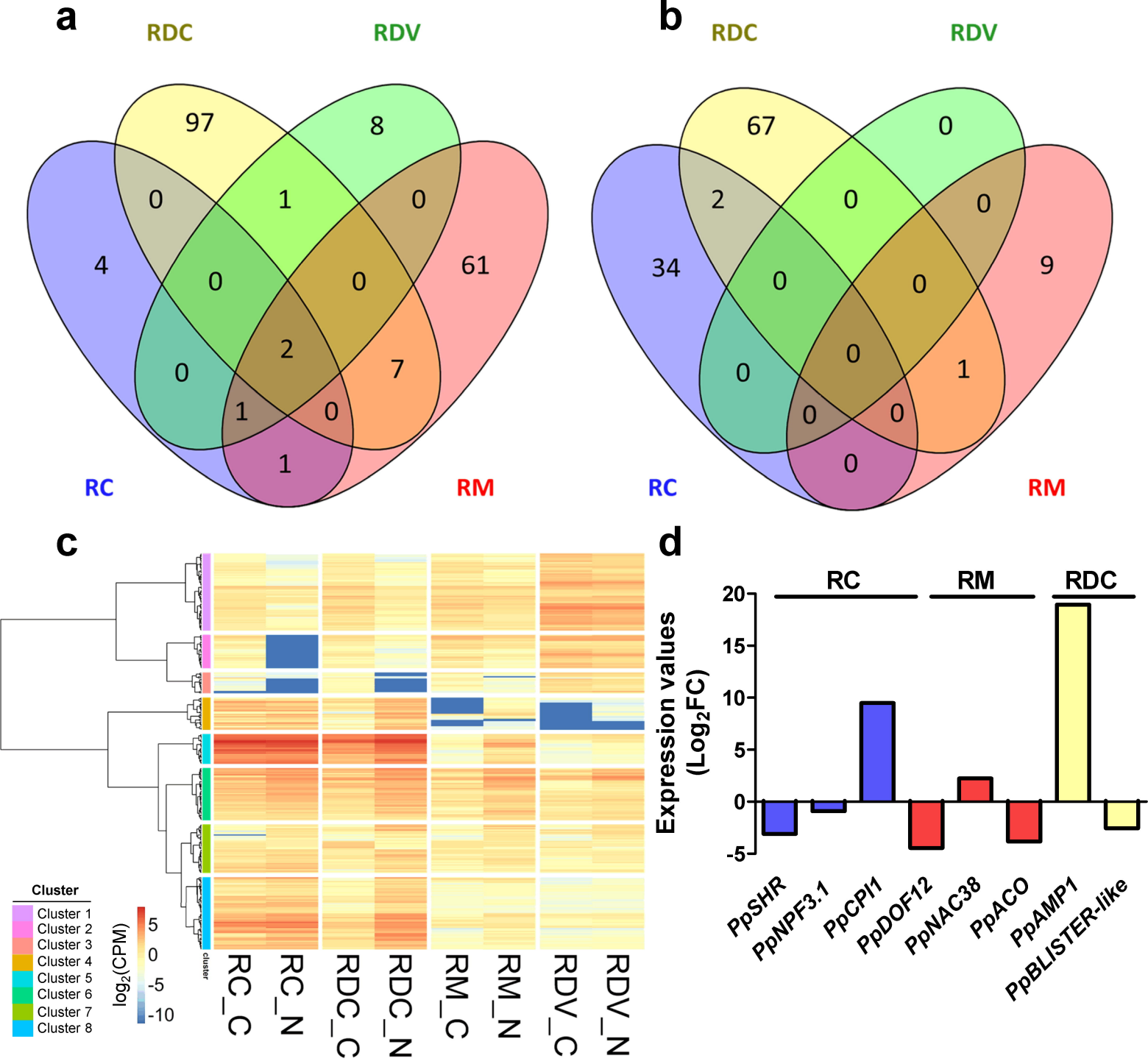

Fig. 2. Low-input RNA-seq results in the different tissues of maritime pine root tip. (**a**) Venn diagram of down-regulated DE transcripts. (**b**) Venn diagram of up-regulated DE transcripts. (**c**) Heatmap and hierarchical clustering of DE transcripts. Expression values correspond to median CPM between biological/experimental replicates. The hierarchical clustering was made employing the Ward's minimum variance method. (**d**) Experimental validation of low-input RNA-seq results for 8 DE transcripts through RT-qPCR. RC, the root cap; RM, root meristem; RDC, root developing cortex; and RDV, root developing vessels. *SHORT-ROOT* (*PpSHR*); *nitrate transporter 1 / peptide transporter family 3.1* (*PpNPF3.1*); *cycloeucalenol cycloisomerase* (*PpCPI1*); *DOF transcription factor 12* (*PpDOF12*); *NAC transcription factor 38* (*PpNAC38*); *aminocyclopropane-1-carboxylic acid oxidase* (*PpACO*); *antimicrobial peptide 1* (*PpAMP1*); *BLISTER-like transcription factor* (*PpBLISTER-like*).

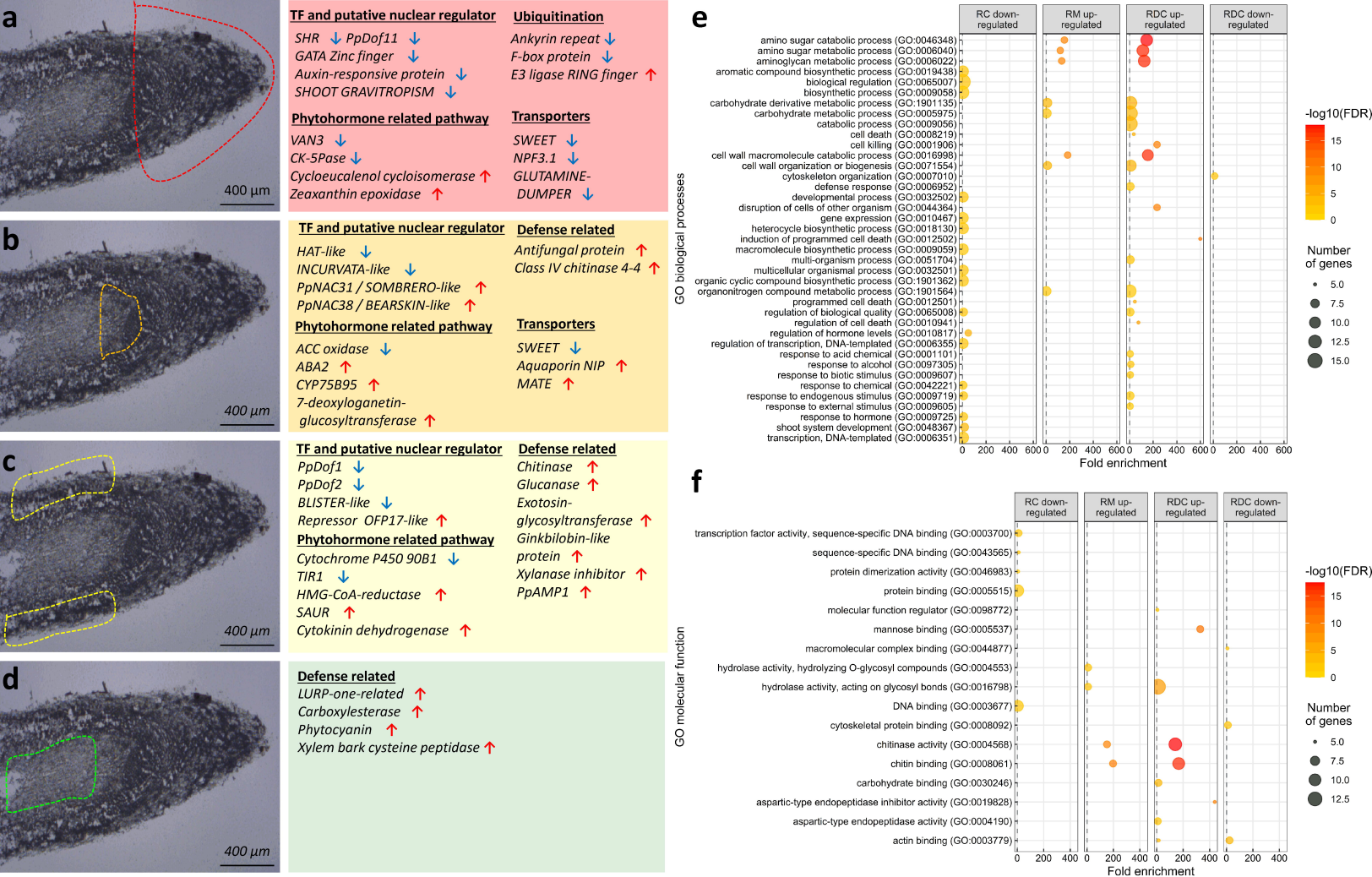

Fig. 3. Resume of the main functional results obtained in the low-input RNA-Seq analysis from LCM isolated samples. Functions and DE transcripts in (**a**) the root cap (RC), (**b**) root meristem (RM), (**c**) root developing cortex (RDC) and (**d**) root developing vessels (RDV). Blue arrows indicate downregulated transcripts, red arrows upregulated ones. (**e**) Significant GO terms from Biological Processes category after a SEA analysis. (**f**) Significant GO terms from Molecular Function category after a SEA analysis.

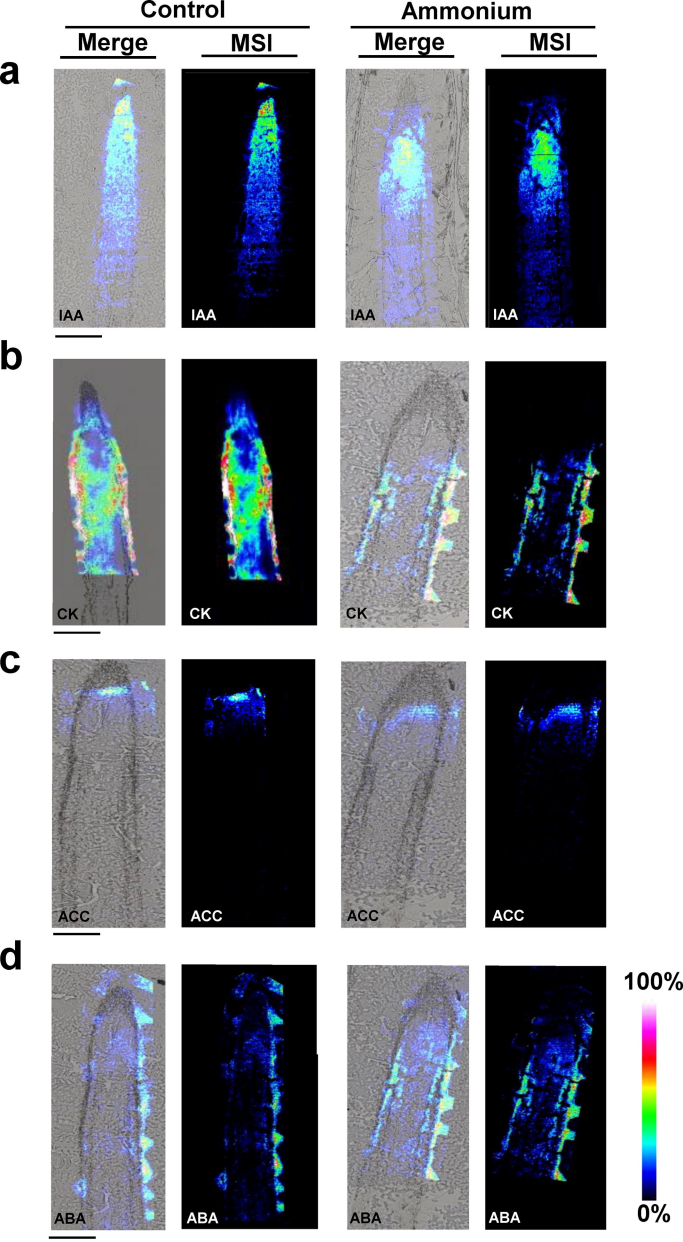

Fig. 4. Phytohormone localization in root apex sections. The main phytohormones were localized in root apex cuts of control and 3 mM NH_4^+ treated seedlings. The phytohormone identification and imaging was made using nano-particle assisted laser desorption/ionization mass spectrometry imaging (Nano-PALDI-MSI). (**a**) Auxin / Indole-3-acetic acid (IAA); (**b**) cytokinin (CK); (**c**) aminocyclopropane-1-carboxylic acid (ACC); (**d**) abscisic acid (ABA). Size bars correspond to 500 µm.

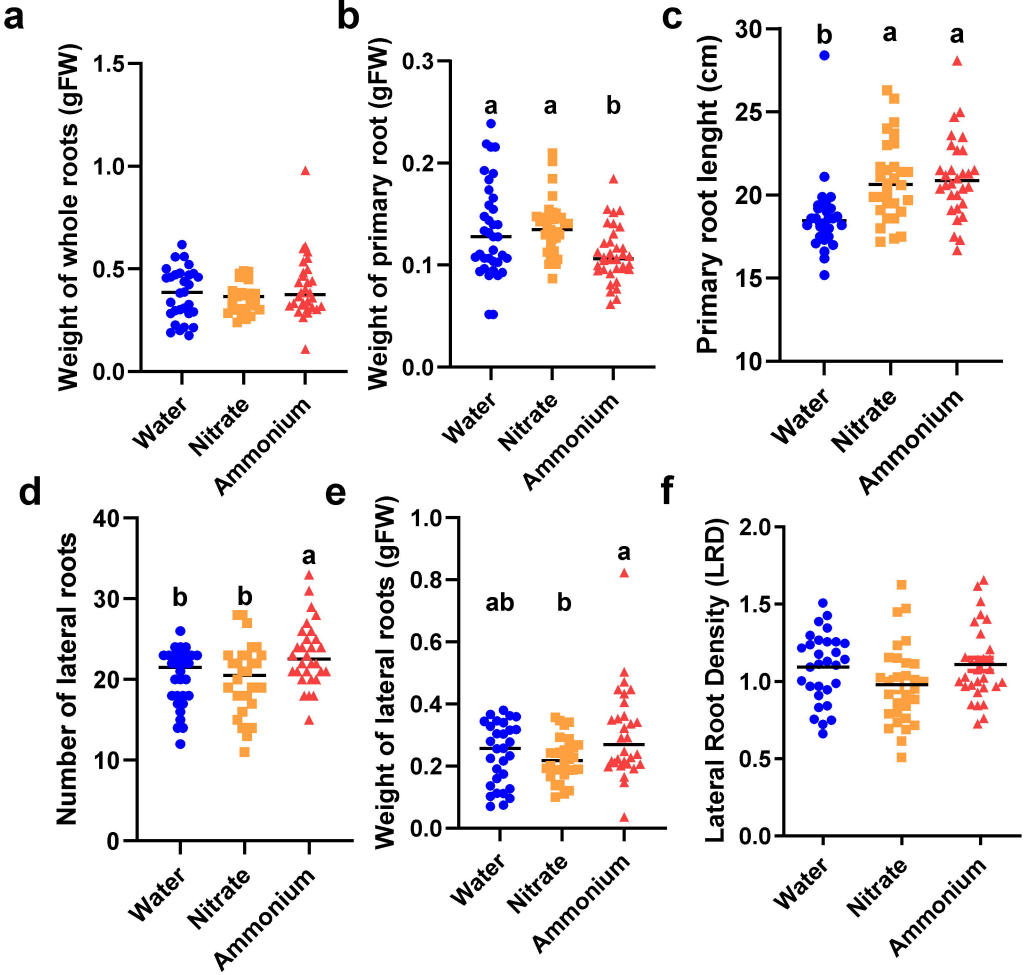

Fig. 5. Root growth and architecture parameters. Pine seedlings were cultivated for 74 days and irrigated once a week with 50 mL of water, 3 mM KNO_3 and 3 mM NH_4Cl, respectively. Six different parameters were measured after harvesting: (**a**) weight of whole roots; (**b**) weight of primary root; (**c**) primary root length; (**d**) number of lateral roots; (**e**) weight of lateral roots; (**f**) lateral root density. Significant differences were determined with a one-way ANOVA. Letters above the conditions show significant differences based on a Turkey post-hoc test ($P < 0.05$) with a n = 30.

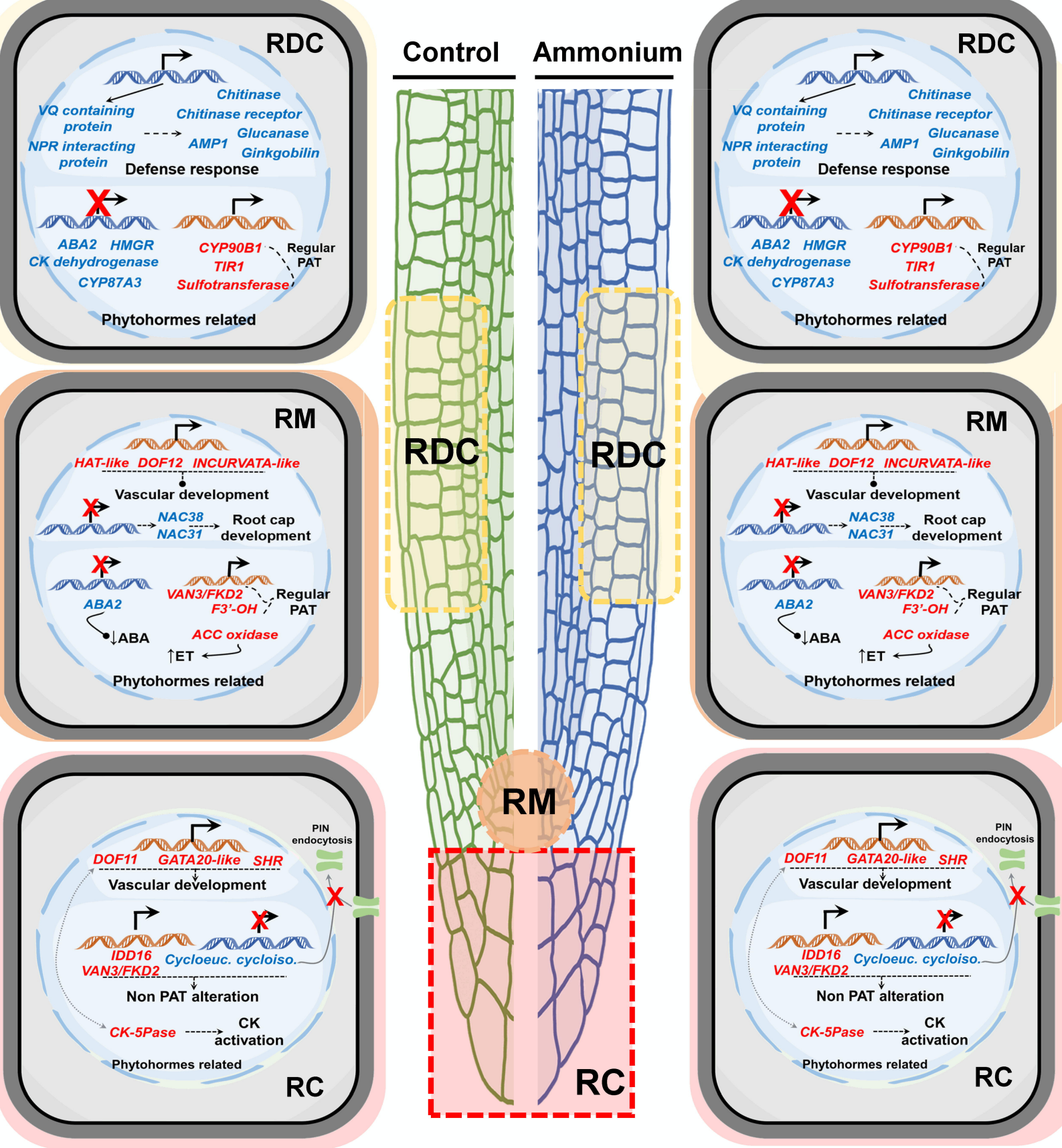

Fig. 6. Schematic representation of the transcriptional response induced by NH_4^+ supply in maritime pine seedling roots 24 h after irrigation. Transcripts in red letters are upregulated. Transcripts in blue letters are downregulated. The root tip tissues are the root cap (RC) root meristem (RM) and root developing cortex (RDC). Results for root developing vessels (RDV) are not shown since they were very limited.